RODRIGO TEIXEIRA AVILA

MANIPULATION OF SOURCE-TO-SINK RATIOS IN GIRDLED COFFEE BRANCHES EVIDENCES LACK OF PHOTOSYNTHETIC DOWN-REGULATION: THE INTERPLAY OF PHOTOSYNTHESIS WITH RESPIRATION AND PHOTORESPIRATION PATHWAYS AND AMINO ACID METABOLISM

Dissertation submitted to Federal University of Viçosa, as part of the requirements for obtaining the *Magister Scientiae* degree in Plant Physiology.

VIÇOSA
MINAS GERAIS – BRASIL
2016

Ficha catalográfica elaborada pela Biblioteca Central da Universidade Federal de Viçosa - Campus Viçosa

T
A958m
2016

Avila, Rodrigo Teixeira, 1987-
Manipulation of source-to-sink ratios in girdled coffee branches evidences lack of photosynthetic down-regulation : the interplay of photosynthesis with respiration and photorespiration pathways and amino acid metabolism / Rodrigo Teixeira Avila. – Viçosa, MG, 2016.
vii, 39f. : il. (algumas color.) ; 29 cm.

Inclui anexos.
Orientador: Fábio Murilo da Matta.
Dissertação (mestrado) - Universidade Federal de Viçosa.
Referências bibliográficas: f.17-24.

1. Café. 2. Análise foliar. 3. Fotossíntese. 4. Aminoácidos - Metabolismo. 5. Metabolismo primário. I. Universidade Federal de Viçosa. Departamento de Biologia Vegetal. Programa de Pós-graduação em Fisiologia Vegetal. II. Título.

CDD 22. ed. 633.73

RODRIGO TEIXEIRA AVILA

MANIPULATION OF SOURCE-TO-SINK RATIOS IN GIRDLED COFFEE BRANCHES EVIDENCES LACK OF PHOTOSYNTHETIC DOWN-REGULATION: THE INTERPLAY OF PHOTOSYNTHESIS WITH RESPIRATION AND PHOTORESPIRATION PATHWAYS AND AMINO ACID METABOLISM

Dissertation submitted to Federal University of Viçosa, as part of the requirements for obtaining the *Magister Scientiae* degree in Plant Physiology.

APPROVED: February 25th, 2016.

Adriano Nunes Nesi	Samuel Cordeiro Vitor Martins
Leandro Elias Morais	Fábio Murilo DaMatta (Adviser)

“Digo: o real não está na saída nem
na chegada: ele se dispõe para a gente
é no meio da travessia”

João Guimarães Rosa

I offer

this accomplishment to my dear family. My parents Jorge and Alaíde and my brother Jorge Luís. You have been teaching me the exact meaning of love over my whole life. My eternal love and gratitude!

ACKNOWLEDGEMENTS

Thanks God for blessing me in every single difficult time and keeping me focused and strong in order to overcome the adversities.

Thanks are due to the Universidade Federal de Viçosa, especially the Plant Physiology Graduate Program, for the availability of its facilities during the development of this work. Thanks are also due to CNPq which has provided me a scholarship in the last two years and the Núcleo de Biomoléculas for providing the facilities to perform the metabolic profiling analyses.

I am indebted to Professor Fábio DaMatta, for his friendship and advising in various development steps of this research project.

Thanks are also due to Professors Adriano, Leandro and Samuel for their excellent suggestions and fruitful collaboration for improving this study.

Thanks to Lilian, Paulo, Matheus, Kelly, Martielly, Lucas, Amanda and Filipe for their help during several steps of my experiments.

Dear friends Álefe and Luis Carlos, “gracias” for everything. Thanks for the support and advices in uncertain times, for their happiness and unmeasured friendship.

Last, but not least, thanks to all colleagues who contributed to this work and were not nominated. My sincerest thanks!

CONTENTS

RESUMO

AVILA, Rodrigo Teixeira, M.Sc., Universidade Federal de Viçosa, Fevereiro de 2016. **Manipulações da razão fonte:dreno em ramos anelados de café evidenciam a ausência de retroinibição à fotossíntese: a interação entre fotossíntese, respiração, fotorrespiração e o metabolismo de aminoácidos.** Orientador: Fábio Murilo da Matta.

No presente trabalho, objetivou-se uma melhor compreensão de como a regulação da fotossíntese em café depende da atividade do dreno e do acúmulo de carboidratos nas folhas-fonte, e de como o cafeeiro ajustaria o seu desempenho fotossintético e o metabolismo primário em resposta a diferentes razões fonte:dreno. Para tanto, utilizou-se de uma abordagem integrativa combinando-se avaliações de trocas gasosas, fluorescência da clorofila *a*, análises de carboidratos e principais metabólitos, atividades de uma gama de enzimas e expressão de alguns genes que codificam para enzimas-chave do metabolismo de carbono, a fim de se ter uma visão holística do metabolismo foliar, em resposta à manipulação de longo prazo da razão fonte:dreno. Para tal, desenhou-se um experimento de campo utilizando-se ramos anelados de café, os quais foram posteriormente manipulados por desfolha e/ou desfrutificação controladas, de maneira a obterem-se três razões fonte:dreno drasticamente distintas. Observou-se que, sob razões fonte:dreno extremamente elevadas, a taxa fotossintética foi limitada principalmente por fatores difusionais (aparentemente sem relação com ácido abscísico em nível de folha inteira), sem sinais aparentes de retroinibição por acúmulo de produtos finais. Tal fato foi associado a uma notável capacidade de acumulação de amido em paralelo à manutenção de níveis baixos de açúcares solúveis. A fotoinibição crônica e ocorrência de danos fotoxidativos puderam ser evitados por meio de ajustes fotoquímicos, bem como na fotorrespiração e respiração, dentre outros processos. Não se observaram evidências consistentes de reprogramação metabólica, em nível de enzimas-chave do metabolismo do carbono. Ajustes metabólicos nas folhas-fonte foram mais evidentes em condições de alta demanda pelos drenos e foram centrados mais sobre o metabolismo do nitrogênio do que sobre o metabolismo de carbono. Em conclusão, os resultados oferecem avanços sobre a alta articulação entre o suprimento e demanda de fotoassimilados em cafeeiros, sem sinais evidentes de retroinibição da fotossíntese, mesmo em condições extremamente baixas de demanda de dreno.

ABSTRACT

AVILA, Rodrigo Teixeira, M.Sc., Universidade Federal de Viçosa, February 2016. **Manipulation of source-to-sink ratios in girdled coffee branches evidences lack of photosynthetic down-regulation: the interplay of photosynthesis with respiration and photorespiration pathways and amino acid metabolism.** Adviser: Fábio Murilo da Matta.

We aimed to gain a better understanding on how the regulation of photosynthesis in coffee depends on sink activity or carbohydrate build-up in source leaves and how the coffee tree adjusts its photosynthetic performance and primary metabolism to varying source-to-sink ratios. For these purposes, we use integrative approaches combining gas-exchange and chlorophyll *a* fluorescence measurements, analyses of carbohydrates and major metabolites, activities of a range of enzymes and the expression of some genes encoding for key enzymes of the carbon metabolism to achieve a holistic view of the whole leaf metabolism in response to long-term source-to-sink manipulation. We designed a field experiment by girdling coffee branches that were further manipulated by controlled defoliation and/or defruiting so that three highly varying source-to-sink ratios were created. We found that under remarkably high source-to-sink ratios photosynthesis rates were chiefly limited by diffusive factors (that were apparently unrelated to whole-leaf abscisic acid) with no apparent signs of feedback down-regulation. Lack of down-regulation was associated with an enormous capacity for starch accumulation coupled with maintenance of low levels of soluble sugars. Chronic Chronic photoinhibition and photodamage could be avoided through adjustments in leaf photochemistry, photorespiration and respiration amongst other processes. No major metabolic reprograming was found at the level of key enzymes associated with carbon metabolism. Metabolic adjustments in source leaves were more evident under high-sink demand conditions and centered more on nitrogen metabolism than on carbon metabolism. In conclusion, our results offer novel insights on the high coordination between the source supply and sink demand in coffee trees, with no evident signs of photosynthetic down-regulation even under dramatically low-sink conditions.

Introduction

A growing body of evidence suggests that photosynthesis and sink utilization of carbohydrates are tightly coordinated (Smith and Stitt, 2007; Ainsworth and Bush, 2011). Overall, photosynthesis in source leaves is up-regulated by sink demand and down-regulated by carbohydrate accumulation (Paul and Foyer, 2001; Paul and Pellny, 2003; Rolland et al., 2006), but the biochemical and molecular mechanisms underlying these processes are not yet fully understood.

Source-to-sink manipulations, e.g. via girdling, defruiting and sucrose-feeding approaches, performed to led to increases in soluble sugars and/or starch pools in leaves, have been shown to down-regulate the photosynthetic process in a range of species (Iglesias et al., 2002; Urban et al., 2004; Franck et al., 2006; Lobo et al., 2015). This feedback inhibition has been associated with decreases in Rubisco expression (particularly the *rbcS*) and other Calvin cycle enzymes with concomitant lower rates of carboxylation and electron transport (Stitt et al., 1991). Accumulation of sugars may directly affect the expression of genes coding for ADP-glucose pyrophosphorylase, an enzyme that catalyzes the rate-limiting step in the starch biosynthetic pathway (Müller-Röber et al., 1994), and genes for other enzymes associated with sucrose and starch metabolism (Koch, 1996). Furthermore, carbohydrate build-up under conditions of limited sink activity may potentially regulate the signaling cascade of plant hormones, which may directly affect physiological processes such as stomatal aperture and leaf senescence (Eveland and Jackson, 2012). In several species, for example, abscisic acid (ABA) has been shown to accumulate in parallel with carbohydrates after girdling treatments, leading to stomatal closure and further compromising the photosynthetic capacity (Xu et al., 2014; López et al., 2015).

Coffee (*Coffea arabica*), an evergreen tropical tree species, is one of the most heavily globally traded commodities. In this species, a high coordination between the activity of source supply and the sink demand has been proposed in several studies. For instance, Cannell (1971) noted lower values of net CO_2 assimilation rate (A) (approx. 30%) when the coffee trees were completely de-blossomed, while Vaast et al. (2005) demonstrated that A was 60% lower in girdled de-fruited branches than in girdled branches bearing a high crop load. Franck *et al.* (2006) observed a negative correlation

between *A* and total soluble sugars and concluded, from sucrose-supplementation approaches, that the photosynthetic down-regulation in leaves from girdled coffee branches is correlated with sucrose levels in the phloem of source leaves. In sharp contrast, studies conducted by our research group demonstrated that sink limitations to photosynthesis are largely mediated by a reduction in stomatal conductance (g_s) and are independent of carbon metabolism (DaMatta et al., 2008). We also observed, in girdled, vegetative branches of coffee saplings a remarkable decrease in *A* and particularly in g_s that were accompanied by increases in starch but not in hexoses and sucrose pools. Furthermore, we noted that the rate of $^{14}CO_2$ uptake (assessed under saturating CO_2 conditions) and the partitioning of recently fixed ^{14}C were not affected by girdling, and concluded that differences in *A* in leaves from girdled and non-girdled branches were merely a consequence of diffusive limitations rather than from direct metabolite-mediated down-regulation of photosynthesis (Batista et al., 2012). Nevertheless, in the above-quoted studies, concentrations of soluble sugars and starch (at most approx. 6% on a leaf dry basis (DW) basis for both soluble sugars and starch) were relatively low, and in some of them (Vaast et al., 2005; Franck et al., 2006) starch pools were unquantified. More recently, we demonstrated, in coffee trees growing under free-air CO_2 enrichment conditions, that starch accumulated at high levels (approx. 11% on DW basis that was accompanied by nearly constant levels of soluble sugars) in leaves with no signs of photosynthetic down-regulation, even during the period of lowest sink demand over the coffee annual growth cycle (DaMatta et al., 2016), when acclimation would be expected to be exceptionally marked.

From the above, whether and how the regulation of photosynthesis in coffee depends on sink activity or carbohydrate build-up in source leaves deserves further studies. Indeed, many gaps within this context remain unresolved. For example, it there would be a carbohydrate threshold that triggers the photosynthetic down-regulation process? Under highly contrasting source-to-sink ratios, how the coffee tree adjusts its primary metabolism and its photosynthetic performance? To gain a better understanding on these subjects, we designed a field experiment by girdling coffee branches that were further manipulated by controlled defoliation and/or defruiting so that three highly varying source-to-sink ratios were created. We use integrative approaches combining gas-exchange and chlorophyll *a* fluorescence measurements, analyses of carbohydrates and major metabolites, activities of a range of enzymes and the expression of some

genes encoding for key enzymes of the carbon metabolism to achieve a holistic view of the whole leaf metabolism in response to long-term source-to-sink manipulation. Our results offer novel insights on the high coordination between the source supply and sink demand in coffee trees, with no evident signs of photosynthetic down-regulation even under dramatically low-sink demand conditions. Additionally, we demonstrated that adjustments in whole-leaf metabolism in response to the varying source-to-sink ratios were associated with respiratory and photorespiratory pathways that in turn seem to be largely coupled with amino acid metabolism.

Material and methods

Plant material and experimental conditions

The experiment was conducted under field conditions with coffee trees cv. 'Catimor', a hybrid derived from a cross between two cultivars: Caturra (*C. arabica* L.) and Timor (*C. arabica* x *C. canephora* Pierre ex Froehner)). The plants, with approximately 6 years of age, were grown as a hedgerow on a Red Yellowish Podzol, in Viçosa (20º45'S, 42º15'W, 650-m altitude), southeastern Brazil. The site is characterized by a subtropical climate with mean annual temperature of 19ºC and receives an average rainfall of 1,200 mm, mainly distributed from September/October to March (growing season). The trees were cultivated in full sunlight and were planted at a spacing of 3.0 x 1.0 m. Routine agricultural practices for commercial coffee bean production, including hoeing, fertilization, irrigation and control of insect and pathogen attack, were used.

In December 2014, trees were selected based on their uniformity and vigor. A lot of plagiotropic (lateral) branches were selected on several coffee trees. For all of the branches analyzed, the fruit number was counted, and the total leaf area was estimated using the maximum leaf widths and lengths and the equations described by Antunes et al. (2008). The selected branches were then managed by removing fruits and/or leaves to achieve three different leaf-to-fruit ratios: completely defruited branches; 20 cm^2 of leaf area $fruit^{-1}$; and 5 cm^2 of leaf area $fruit^{-1}$. These treatments represented, respectively, high, intermediate and low source-to-sink ratios (hereafter referred to as HSS, ISS and LSS, respectively). The ISS treatment was based on the results of Cannel (1976) that a leaf area of 20 cm^2 is required to support the normal development of each coffee fruit without compromising the vegetative growth of coffee branches.

Given that branch autonomy is relatively low in coffee, particularly under high-sink demand conditions (Chaves et al., 2012), we used girdling as an experimental approach to avoid confounding effects associated with assimilate redistribution within the coffee tree (see DaMatta et al., 2008). All of the selected branches were then carefully ring-barked at their base by entirely removing the bark (2-cm wide). The exposed tissues were protected with a PVC film to avoid drying and to prevent insect and pathogen attack. Expanding leaves near the branch apex were eliminated to avoid sink effects and exacerbate the accumulation of carbohydrates (especially in the HSS treatment).

All of the samplings and measurements were performed on completely expanded leaves from the third or fourth leaf pair from the apex of plagiotropic branches on clear-sky days in January 2015 (bean-filling stage when demand for assimilates by the fruit is greatest). Unless otherwise indicated, gas exchange and chlorophyll *a* fluorescence parameters were measured during three time periods: 08:00-09:00 h, 11:30-12:30 h, and 15:30-16:30 h (solar time). For biochemical analyses, leaf tissues were collected at five time points (approximately at 06:00, 12:00, 18:00, 00:00 and 06:00* h (*next day morning) and then flash frozen in liquid nitrogen with subsequent storage at -80 ºC until analysis. Based on preliminary evaluations, all of these samplings and analyses were conducted at 10 days after girdling when the net carbon assimilation rate (*A*) was remarkably depressed in parallel with strong starch accumulated but with no signs of leaf senescence, as found in the HSS treatment.

Gas exchange and chlorophyll a *fluorescence parameters*

The gas exchange parameters [*A*, g_s and internal CO_2 concentration (C_i)] were measured simultaneously with chlorophyll *a* fluorescence parameters using two cross-calibrated portable infrared gas analyzers [model LI-6400XT (Li-COR Biosciences INC., Nebraska, USA) equipped with integrated fluorescence chamber heads (model LI-6400-40, Lincoln, NE, USA)]. Measurements were carried out at the leaf level at an artificial photon irradiance of 1000 µmol m^{-2} s^{-1} and 40 Pa partial pressure of CO_2. Further details have been described elsewhere (DaMatta et al., 2016).

At predawn, the minimum fluorescence (F_0) was measured using a weak modulated measuring beam (0.03 µmol photons m^{-2} s^{-1}). Subsequently, the maximal fluorescence (F_m) was measured by applying a saturating actinic light pulse (8000 µmol photons m^{-2} s^{-1}) for 0.8 s. Using these parameters, the variable-to-maximum

fluorescence ratio, $F_v/F_m = [(F_m - F_0)/F_m)]$ was calculated. In light-adapted leaves, the steady-state fluorescence yield (F_s) was measured after registering the gas exchange parameters. A saturating white light pulse (8,000 μmol m^{-2} s^{-1}; 0.8 s) was applied to achieve the light-adapted maximum fluorescence (F_m'). The actinic light was then turned off, and far-red illumination was applied (2 μmol m^{-2} s^{-1}) to measure the light-adapted initial fluorescence (F_0'). Using the values of these parameters, the coefficient for photochemical quenching (q_P) was calculated as $q_P = (F_m' - F_s)/(F_m' - F_0')$, and the coefficient for non-photochemical quenching (NPQ) was calculated as NPQ = (F_m/F_m') – 1. The actual quantum yield of PSII electron transport (Φ_{PSII}) was obtained as $\Phi_{PSII} = (F_m' - F_s)/F_m'$, from which the apparent electron transport rate (ETR) was calculated as ETR = Φ_{PSII}*PPFD*f*α, where f is a factor that accounts for the partitioning of energy between PSII and PSI and is assumed to be 0.5, which indicates that the excitation energy is distributed equally between the two photosystems, and α is the leaf absorptance by the photosynthetic tissues and is assumed to be 0.84 (Maxwell and Johnson, 2000).

The rate of mitochondrial respiration in darkness (R_D) was measured at midnight and used to estimate light respiration (R_L) according to Lloyd et al. (1995) as $R_L = (0.5 - 0.05\ln(PPFD))R_d$. The photorespiratory rate of Rubisco (R_p) was calculated as $R_P = 1/12[ETR - 4(A + R_L)]$ according to Valentini et al. (1995), after which the photorespiration-to-gross photosynthesis ratio (R_P/A_{gross}) ratio was obtained throughout the day by computing the values of R_P, A and R_L, as described elsewhere (DaMatta et al., 2016). Additionally, single-point maximum apparent carboxylation capacity on a chloroplastic CO_2 concentration basis (V_{cmax}) was estimated following the methodology described elsewhere (Wilson et al., 2000; De Kauwe et al., 2016), using the kinetic properties of Rubisco determined for coffee [as reported in Martins et al. (2013)] and the values of A and ETR measured at 08:00 h (when both A and g_s are at their maxima).

Pyridine nucleotides

Nucleotide extraction was performed by grinding the lyophilized leaf materials with liquid nitrogen and immediate addition of the appropriate extraction buffers. The levels of NAD(H) and NADP(H) were spectrophotometrically determined based on the selective hydrolysis of NAD(P)H in acid medium, and of $NAD(P)^+$ in alkaline medium, exactly as described in Gibon et al. (2004).

Metabolites

Leaf samples were lyophilized at -48°C and crushed in a ball mill. A 10 mg sample of ground tissue was added to pure methanol, and the mixture was incubated at 70°C for 30 min. After centrifugation (16,200 x *g,* 5 min), the concentrations of hexoses (glucose plus fructose), sucrose and total amino acids in the supernatant, and starch and proteins (Bradford method) from the methanol-insoluble pellet, were quantified as previously detailed (Praxedes et al., 2006; Ronchi et al., 2006). The levels of nitrate and malate were spectrophotometrically determined using the methanol-soluble phase exactly as reported elsewhere (Nunes-Nesi et al., 2007).

All other metabolites were quantified in lyophilized tissues by an established gas chromatography mass spectrometry (GC-MS)–based metabolic profiling exactly as described by Lisec et al. (2006). Peak detection, retention time alignment, and library matching were performed using Target Search R-package (Cuadros-Inostroza et al., 2009). Metabolites were identified in comparison to database entries of authentic standards (Kopka et al., 2005; Schauer et al., 2005). Identification and annotation of detected peaks followed the recommendations for reporting metabolite data described in Fernie et al. (2011).

Enzymatic activity profile

Enzyme extracts were prepared as described by Nunes-Nesi et al. (2007). The activity of the following enzymes were quantified: NAD^+-dependent malate dehydrogenase (NAD^+-MDH), sucrose synthase (SuSy); ribulose-1,5-bisphosphate carboxylase-oxygenase (RuBisCO) (Sulpice et al., 2007); ADP-glucose pyrophosphorylase (AGPase) (Tiessen et al., 2002); triose-phosphate isomerase (TPI), hexokinase (HK), enolase (ENO), NADPH-dependent glyceraldehyde 3-phosphate dehydrogenase (NADPH-GA3PDH) (Fernie et al., 2001); aldolase (ALD), phosphoglycerate kinase (PGK), phosphofructokinase (PFK) (Gibon et al., 2004); acidic and alkaline invertase (Praxedes et al., 2006; Ronchi et al., 2006) and sucrose-6-phosphate synthase (SPS) (Jenner et al , 2001). The activation state (%) of both the SPS and RuBisCO was calculated as their initial-to-total activity ratios.

Quantitative real-time PCR

Specific primers were designed to study the expression of genes coding the following enzymes: RuBisCO (small and large subunits), AGPase, SuSy, SPS and invertase (acidic, alkaline and vacuolar) by real-time polymerase chain reaction (RT-QPCR). The sequences of genes of interest were obtained through two databases, Coffea Genome Network and Sol Genomics Network. The designed primers are shown in Supplementary Table S1. RNA extraction was performed according to the methodology described by Fortunato et al. (2010). The integrity of the RNA was checked on 1% (w/v) agarose gels, and the RNA concentration was spectrophotometrically measured before and after DNase I digestion. Digestion with DNAse I (Amplication Grade DNAse I, Invitrogen) was performed according to the manufacturer's instructions. Subsequently, total RNA was reverse transcribed into cDNA using a SuperScript III First-Strand Synthesis SuperMix for qRT-PCR (Invitrogen). The PCR program was as follows: 95°C for 3 min, and 40 cycles of 95°C for 10 s, 65°C for 15 s, and 72°C for 15 s. For the analysis of gene expression, real time PCR (Step One PlusTM Real Time PCR System, Applied Biosystems, CA, USA) with the SYBR green fluorescence detection (Applied Biosystems1) system was employed, using the Platinum1 SYBR1 Green qPCR SuperMix-UDG with ROX kit. The transcription abundance was calculated by the standard curves of each selected gene and normalized using the constitutively expressed coffee actin, with the following primers: forward (5'-TGCTAGTGGTCGGACAACAGGTATAG-3') and reverse (5'-AGTCAAGACGGAGGATGGCATGTG-3'). The determination of the target gene expression levels was calculated by 2-ΔΔCT method (Livak and Schmittgen, 2001).

Statistical analysis

The data obtained were analyzed using a completely randomized design. A 3x3 factorial (three source-to-sink ratios and three evaluation times for gas exchange and chlorophyll *a* fluorescence analyses) or a 3x5 factorial (three source-to-sink ratios x five evaluation times for biochemical/molecular analyses) was used. The data were submitted to an analysis of variance, and the means were compared using the Tukey's test at 5% probability using the Statistical Analysis System (SAS).

Data from the metabolite profiling were firstly normalized by ribitol and dry mass. Secondly, each individual observation was normalized by a general mean (all

treatments and time-points) calculated for each metabolite. Subsequently, data were analyzed by carrying out a clustering analysis of a false heat maps using the software MultExperiemnt Viewer (MeV). For this purpose, an internal tool called Cluster Affinity Search Technique (CAST) was employed, which uses Pearson Correlation to group the metabolites (with a threshold of 0.8) by the same behavior between treatments and time points (Ben-Dor et al., 1999). Means for each metabolite were compared overtime using the Tukey's test as described above.

Results

Varying source-to-sink ratios were linked to changes in gas-exchange rates and adjustments in leaf photochemistry

Regardless of treatments, both g_s and A peaked in the early morning and decreased progressively throughout the day, reaching their minima in the late afternoon. Daily fluctuations in g_s and A, especially from 08:00 to 12:00 h, were sharper in both HSS and ISS leaves than in LSS leaves. Differences in g_s and A across treatments were more evident at 12:00 h, with higher g_s and A values in the LSS leaves than in their ISS and HSS counterparts, which did not differ to one another (Fig. 1A, B). Indeed, LSS leaves, regardless of time-point evaluations, displayed the highest A, with diurnally integrated values of 6.2 μmol CO_2 m^{-2} s^{-1}, against 3.7 and 2.6 μmol CO_2 m^{-2} s^{-1} in the ISS and HSS leaves, respectively. Notably, A correlated positively with g_s ($r^2 = 0.95$, $P < 0.05$) (Fig. 1C). Independently of treatments, C_i was nearly invariant throughout the day (Fig. 1D). The R_P/A_{gross} ratio was similar amongst treatments at 08:00 h, and then increased onwards, but more in HSS and ISS (which did not differ to each other) than in LSS leaves; at 12:00 h, for example, that ratio was 40% higher for HSS and ISS than in LSS leaves (Fig. 1E). We additionally observed that V_{cmax} remained invariant regardless of treatments, whereas R_D was similar in HSS and ISS, but significantly higher (~30%) in comparison to LSS leaves (Fig. 1F, G).

Over the course of the day, q_p remained unchanged in both HSS and ISS leaves; these leaves showed lower q_p values than those from LSS leaves at 08:00 and 12:00 h (Fig. 2A). NPQ, in turn, increased from 08:00 to 12:00 h in both HSS and ISS leaves (40% and 47%, respectively) and then decreased, whereas in LSS no significant diurnal change in NPQ was found. At 12:00 h, the values of NPQ were significantly higher in

HSS and ISS (which did not differ to one another) than in LSS leaves (Fig. 2B). Adjustments in leaf photochemistry led to decreases in ETR throughout the day: in ISS and HSS leaves these decreases occurred from 8:00 to 12:00 h (30% and 40%, respectively) and thereafter remained invariant; in LSS leaves ETR reduction (29%) occurred only from 12:00 to 16:00 h (Fig. 2C). In any case, LSS leaves always displayed higher ETR values than the HSS and ISS leaves (Fig. 2C). In contrast to other chlorophyll *a* fluorescence parameters, F_v/F_m ratio did not differ significantly among treatments and remained above 0.8 for all measurements (data not shown).

Pyridine nucleotide pools varied only marginally across treatments

Overall, minor differences in the pools of pyridine nucleotides were noticeable among treatments. Little, if any, variations in NAD^+, NADH and $NADP^+$ pools were observed among treatments while NADPH pools were consistently higher in LSS than in ISS and HSS leaves. The $NAD(P)H/NAD(P)^+$ ratios in both HSS and ISS leaves were similar to or below those found in LSS leaves (Fig. 3).

Modification in source-to-sink ratios affected mostly the starch and secondarily the amino acid levels coupled with minor changes in the soluble sugars and protein contents

Starch accumulated remarkably with increasing source-to-sink ratios. In HSS leaves, diurnally integrated starch concentrations averaged on 15% on DW basis; these concentrations were 34% and 1080% higher than those in ISS and LSS, respectively (Fig. 4A). Sucrose levels, over the course of the day, fluctuated only slightly in both HSS and ISS leaves, whereas in ISS leaves a clear sucrose turnover was observed, with increases (100%) from 06:00 to 12:00 h and corresponding decreases overnight (Fig. 4B). Hexoses (glucose plus fructose) concentrations, that were remarkably lower than sucrose concentrations, did not differ significantly among treatments along the day (Fig. 4C). Notably, total soluble sugars (sucrose plus hexoses) concentrations did not exceed 3.1% on a leaf DW basis irrespective of treatments. Overall, total amino acid levels did not differ between HSS and ISS (with the exception at 12:00 h) and was consistently higher in leaves from these treatments than in their LSS counterparts (significant in three time points) (Fig. 4D). It should be noted that the overall higher concentration of amino acids in HSS and ISS leaves were coupled with no modifications of total N concentration among the treatments (data not shown).

Protein levels also fluctuated only slightly over the course of the day. The most notable change took place at 18:00 h when the LSS leaves displayed a higher (~20%) protein content than had the HSS and ISS leaves. In any case, in contrast to HSS and ISS, LSS leaves showed a protein turnover of 8% throughout the day (Fig. 4E).

Changes in carbon metabolism enzymes were restricted to AGPase

Overall, activities of a range (14) of key enzymes associated with carbon (C) metabolism, including Calvin-cycle enzymes (RuBisCO, PGK, NADPH-GA3PDH and TPI), sucrose-metabolizing enzymes (SPS, SuSy and invertases) and respiratory enzymes (ENO, PFK, ALD and NAD^+-MDH), remained invariant irrespective of treatments (Table 1, Fig. 5, Fig. S1). The single exception was AGPase. The HSS and ISS leaves displayed higher total AGPase activities than the LSS leaves, ranging from 53% to 192% depending on the time point considered (Fig. 5A). In addition, activation states of both RuBisCO and SPS were also unresponsive to the treatments (Table 1, Fig. 5D).

Relatively minor differences in transcript abundance of some carbon metabolism enzymes were observed in response to varying source-to-sink ratios

Overall, transcript abundance for AGPase, RuBisCO (small and large subunits), SuSy and SPS tended to peak at 12:00 h. At this time point, AGPase transcript abundance was more than three times higher in both the HSS and ISS leaves than in the ISS leaves; at 18:00 h AGPase transcript levels increased with rising source-to-sink ratios (Fig 6A). RuBisCO transcript abundance did not differ among treatments, with a single exception at 12:00 h in which transcripts for the small subunit were less abundant in HSS leaves than in their ISS and LSS counterparts (Fig. 6B-C). For both SPS and SuSy, the most notable differences among treatments were observed at 12:00 h, with transcript abundance increasing in the following order: HSS<LSS<ISS (Fig. 6D-E). Relative expression of cell wall invertases was consistently higher (at 06:00 and 12:00 h) in ISS leaves than in the leaves from the other treatments (Fig. 6F). There were no consistent differences in transcript abundance for both vacuolar and alkaline invertases among the treatments (Fig. 6G-H).

Clustering analysis reveals varying patterns of metabolite fluctuation over the course of the day

To obtain an overview of the major routes of primary metabolism, the full data obtained from GC-MS-based metabolic profiling was displayed in false color heat map; these data with corresponding statistics are additionally shown in the Supplementary Table S2. We successfully annotated a total of 56 metabolites that were used for further CAST analyses, allowing us to obtain a total of 23 clusters. For a better understanding, five of the more relevant clusters (that comprise a minimum of three metabolites with relevant differences among treatments) are presented (Fig. 7), as described as follows: (i) Cluster I is exclusively characterized by amino acids (10) with a consistent turnover pattern throughout the course of the day, with much more marked alterations with decreasing source-to-sink ratios. Indeed, the ISS leaves and especially their LSS counterparts displayed remarkable depressions in the levels of amino acids at 12:00 h and particularly at 18:00 h with an overall recovery onwards. Also importantly, at 12:00 h serine levels were lower in LSS leaves than in leaves from the other treatments; (ii) Cluster II clearly shows a decrease of carbohydrate levels throughout the night and a rising throughout the morning in LSS leaves in contrast with HSS and ISS leaves in which carbohydrates remained nearly invariant; (iii) Cluster III denotes accumulation of glycine and glutamine at 12:00 h, particularly in both the HSS and ISS leaves; (iv) Cluster IV evidences accumulation of succinate and 2-oxoglutarate at 12:00 h, but only in the LSS leaves; (v) Cluster V is characterized by grouping metabolites which, irrespective of the time points evaluated, had higher relative contents with increasing source-to-sink ratios. Basically, these metabolites are mainly amino acids (alanine, proline, aspartate and asparagine), oxaloacetate and two sugar alcohols (galactinol and glycerol). Overall, metabolic profiles suggest that amino acids presented higher relative levels with rising source-to-sink ratios, which largely agrees with the total amino acid concentrations (Fig. 4D). Despite not being grouped in any of the five above-mentioned clusters, it deserves attention the fact that the levels of fumarate and malate, on most time points, were higher (coupled with lower levels of oxaloacetate, alanine and aspartate; cluster V, Fig. 7) in LSS leaves than in HSS and ISS leaves (Fig. 6).

Discussion

Our experimental approach was proven to be successful to produce highly contrasting source-to-sink ratios that were largely contrasted to each other by clear differences in starch accumulation with minor changes in soluble sugars. However, differences in starch accumulation between HSS and ISS leaves were narrower than previously expected, possibly because vegetative growth was restrained by removing the expanding leaves. Irrespective, we intended, on the one hand, to induce starch to be accumulated as much as possible and, to the best of our knowledge, starch reached concentrations that are the greatest so far measured in coffee. Under these circumstances end-product-mediated down-regulation of photosynthesis is expected to be marked. Nevertheless, as evidenced below, signs of photosynthetic down-regulation were not found. On the other hand, under high-sink demand, A was up-regulated via enhanced g_s, as also previously observed in ungirdled coffee branches (DaMatta et al., 2008). Essentially, we here provide novel evidence reinforcing the high coordination between the source supply and sink demand in coffee trees. Adjustments in whole-leaf metabolism to cope with these contrasting source-to-sink ratios, especially in the respiratory and photorespiratory pathways coupled with amino acid metabolism, are discussed with respect to current models of metabolic regulation.

Under remarkably high source-to-sink ratios photosynthesis rates are chiefly limited by diffusive factors with no apparent signs of feedback down-regulation

Our data clearly suggest that A was largely limited by diffusional factors whereas the biochemical capacity to fix CO_2 was preserved. Compelling evidence for this comes from the strong correlation between A and g_s, and invariant V_{cmax} on a chloroplastic CO_2 concentration basis coupled with unchanging RuBisCO activity and activation state. The decreases in g_s played, therefore, a key role in governing the depressions in A in the HSS and ISS leaves. We cannot dismiss that a decreased mesophyll conductance also played a pivotal role in this regard given that both stomatal and mesophyll conductances are often highly correlated over a range of conditions (Flexas et al., 2012), as also observed in coffee seedlings (Martins et al., 2014). Irrespective, g_s was apparently unrelated to changes in both C_i and whole-leaf ABA contents (estimated in leaf samples collected at 12:00 h using an LC/MS system; data not shown). However, we cannot discard a role of ABA in governing the responses of g_s to source-to-sink imbalances given that we do not measure ABA in guard cells (Zhang

and Outlaw, 2001; Wilkinson and Davies, 2008). The exact mechanism by which g_s responds to source-to-sink imbalances in coffee remains to be resolved in future studies.

The lower levels of transcripts of the gene coding for the RuBisCO small subunit (found only at 12:00 h in HSS leaves) might be, at a first glance, and evidence of photosynthetic down-regulation. However, this was not apparently associated with changes in both sucrose and hexoses (Fig. 4B-C) and, in addition, the unchanged V_{cmax} and RuBisCO activity and activation state argue against occurrence of photosynthetic down-regulation (Stitt et al., 1991; Ainsworth and Long, 2005). Irrespective, our data also suggest a striking ability of coffee leaves to synthetize (via higher transcription coupled with higher activity of AGPase) and accumulate starch at high levels when the sink demand is severely compromised while maintaining a relatively low total soluble sugar concentration (Fig. 4). This information is consistent with the suggestion of DaMatta et al. (2016) that increased starch levels under sink limitations, instead of feeding back to decrease photosynthetic performance, allow the coffee leaves to avoid photosynthetic down-regulation; this would prevent the cycling and/or accumulation of soluble sugars that otherwise could more directly repress photosynthetic gene expression (Paul and Foyer, 2001; Paul and Pellny, 2003) and thereby provoking acclimation. Additionally, the increases in both photorespiration and respiration under sink limitations (Fig. 1E-G) may play a key role in using the surplus of soluble sugars that cannot promptly be used in other metabolic processes, which ultimately would help to buffer their concentrations and further avoiding photosynthetic down-regulation.

Chronic photoinhibition and photodamage could be avoided through adjustments in leaf photochemistry and (photo)respiration amongst other processes

Given that *A*, which often represents the main sink for absorbed light in chloroplasts, decreased significantly with increasing source-to-sink ratios, adjustments of light capture, use and dissipation are required to provide photoprotection to the photosynthetic apparatus. Here, we found that depressions in *A* were accompanied by concordant adjustments in leaf photochemistry, as denoted by decreases in the fraction of absorbed light that is dissipated photochemically (estimated as q_P) together with increases in that fraction that is dissipated thermally (estimated as NPQ). These adjustments were accompanied by decreases in ETR (Fig. 2), thus diminishing the excitation pressure on photosystems. Additionally, the increases in R_P/A_{gross} ratio imply that photorespiration should have acted as a key pathway for dissipating excess energy.

These increases are consistent with the higher levels of glycine, serine and glutamine, which are directly involved in or closely associated with photorespiratory metabolism (Florian et al., 2013), as found at 12:00 h in both HSS and ISS leaves relative to their LSS counterparts. The higher levels of aspartate and alanine in HSS and ISS leaves seem also to be consistent with increased photorespiration rates (see Novitskaya et al., 2002). Regarding to respiration, the higher rates in HSS and ISS leaves may imply in consuming excess carbohydrates that might occur through less energy (ATP) producing respiratory routes (e.g., using alternative NADH dehydrogenase and oxidases, uncoupling protein), thus using more substrate for a given amount of energy released (van Dongen et al., 2011). Indeed, the higher R_D in both HSS and ISS leaves is consistent with our metabolite data, especially at 12:00 h when differences in abundance of the tricarboxylic acid (TCA) cycle intermediates were more evident among treatments (Fig. 6, 7). In those leaves, compared with their LSS counterparts, there were higher levels (at 12:00 h) of both citrate (earlier TCA cycle intermediate) and oxaloacetate (final TCA cycle intermediate) coupled with down-regulation in the levels of several other intermediates such as 2-oxoglutarate, succinate, fumarate and malate (except in ISS leaves), suggesting that the TCA cycle run at higher rates.

Other mechanisms may also contribute to provide protection to the cells under high source-to-sink ratios. For example, there was a greater relative abundance of polyols such as galactinol, and amino acids such as proline (particularly in HSS leaves), which have been revealed to protect plants at least in part through scavenging reactive oxygen species (Nishizawa et al., 2008; Obata and Fernie, 2012). Other alternative pathways, such as the Mehler-peroxidase reaction (Logan et al. 2006; Foyer and Shigeoka 2011), could also have played a role in dissipating the excess reducing power under elevated source-to-sink ratios, as has been shown in coffee under stressful conditions (e.g., Fortunato et al., 2010; Pompelli et al., 2010). Altogether, all of the above described mechanisms are likely to interact to avoid the accumulation of reducing equivalents and, ultimately, oxidative stress under the remarkable photosynthetic limitations associated with the low sink demand. Regardless of these mechanisms, it should be noted that the lower (or similar) NAD(P)H/NAD(P)$^+$ ratios in both HSS and ISS leaves than in the LSS leaves (Fig. 3) implies that redox potentials did not shift toward oxidizing directions (Scheibe et al., 2005), thereby avoiding the creation of an oxidized environment that could potentially lead to the occurrence of oxidative stress with increasing source-to-sink ratios. Indeed, despite the depressions in A no apparent

light-induced symptoms of oxidative stress could be detected, as illustrated by the high F_v/F_m values. In this context, an interplay of the photosynthetic machinery with the metabolic activities in both mitochondria and chloroplasts seems to play important roles for the proper maintenance of intracellular redox gradients to allow for considerable rates of energy use and dissipation with increasing source-to-sink ratios.

No major metabolic reprograming was found at the enzyme level

We previously expected an extensive reorchestration of the central metabolism in response to our contrasting treatments. For example, we expected significant changes in the expression patterns of genes coding for sucrose-metabolizing enzymes given that sucrose synthesis and export are often profoundly affected by imbalances in source-to-sink relationships (Rolland et al., 2006). However, there were only a few alterations in transcript levels of these enzymes; additionally, the relative abundance of their transcripts changed apparently inconsistently among treatments over the course of the day. Most importantly, regardless of source-to-sink ratios, activities of sucrose-metabolizing enzymes (as well as some enzymes associated with photosynthesis and respiration) remained unaltered, suggesting that post-transcriptional regulations on these enzymes occurred in this study. It is tempting, therefore, to speculate that metabolism achieved a considerable homeostasis with subtle alterations at the level of the key pathway enzymes (Piques et al., 2009) associated with C metabolism.

Metabolic adjustments in source leaves occurred mostly under high-sink demand conditions and was centered more on nitrogen metabolism than on carbon metabolism

The feed-forward stimulation on *A* at low source-to-sink ratios seems to be not sufficient to sustain the proper development of coffee fruits when the crop burden exceeds certain limits. Under these circumstances, an overall depression of carbohydrates can occur and, as a consequence, fruit filling can be seriously compromised (DaMatta et al., 2008; Chaves et al., 2012). Our data suggest that, under these high-sink demand conditions, the protein turnover, as noted in LSS relative to ISS and HSS leaves (Fig. 4E), might be an attempt of the coffee plant to guarantee a proper development of fruits which are by far the priority sinks in coffee (DaMatta et al., 2010). Indeed, protein degradation has been shown to be increased under carbon starvation, and the resulting amino acids can be directed towards the respiratory metabolism as an alternative carbon source (Araujo et al., 2011; Izumi et al., 2013). This seems to be the case of this study given that protein turnover was accompanied by

unchanged total amino acid levels (Fig. 4D). Indeed, the increases in branched-chain amino acids (leucine, isoleucine and valine) and aromatic amino acids such as phenylalanine at 00:00 h relative to 18:00 h (cluster I; Fig. 7) might suggest an increased proteolysis and the use of these amino acids as alternative respiratory substrates (Florian et al., 2013; and references therein). .

Notably, our metabolite profiling data reveal important features associated with assimilate export under high-sink demand. For example, by comparing LSS with HSS leaves, the former always displayed lower levels of total amino acids (but not N) which is indicative of a greater export of N compounds towards the developing fruits given that up to 95% of total plant N can be taken up by fruits in heavily bearing coffee trees (Cannell, 1975). Asparagine is by far the major form of N that is transported in coffee (Mazzafera and Gonçalves, 1998). Taken together, this information strongly suggests that the remarkable depression in asparagine pools in LSS leaves (cluster V; Fig. 7) should precisely represent increased export rates rather than decreased synthesis. Although we do not perform any measurement of metabolic fluxes across biochemical pathways, it is tempting to suggest that the TCA cycle operated in a non-cyclic way by deviating oxaloacetate pools to ultimately allow higher rates of synthesis of asparagine. Evidence to this comes from the higher malate levels in parallel with a strong depression in the levels of oxaloacetate, whereas the levels of aspartate, which is linked to malate via oxaloacetate, malate dehydrogenase and amino transferase activities (Florian et al., 2013), were generally depressed (cluster V, Fig. 7).

Our metabolomic analysis also revealed relatively minor changes in carbohydrate pools in contrast to what occur with both organic acids linked to the TCA cycle and especially amino acids (with stronger alterations in LSS leaves), whereas the levels of the remaining metabolites differed, in general, minimally across treatments. Taken all of the above information together, our data suggest that a relative cellular homeostasis associated with C metabolism, but not with N metabolism, was maintained irrespective of source-to-sink imbalances. Inasmuch as several intermediates of the TCA cycle contribute to provide carbon skeletons to amino acid biosynthesis, we contend that variations in abundance of these intermediates might be more related to anaplerotic reactions associated with N metabolism (as exemplified above with asparagine) rather than with changes in cell energetics *per se*.

Conclusion

For obvious reasons, leaf carbohydrates cannot increase infinitely. Here, we forced the plants to accumulate starch as much as possible and, even so, no photosynthetic down-regulation associated with the enormous starch amounts was apparently triggered. In parallel, the plants kept relatively low soluble sugar levels, which are believed to be a key feature to prevent such a down-regulation. Adjustments in both respiration and photorespiration rates might play important roles to help the plant to maintain low soluble sugar levels; in addition these adjustments should also contribute to proper maintenance of intracellular redox gradients to allow for considerable rates of energy use and dissipation with increasing source-to-sink ratios. Our data suggest that a relative cellular homeostasis associated with C metabolism was achieved regardless of source-to-sink imbalances. In contrast, extensive alterations in N metabolism were evident, particularly under high-sink demand conditions. We believed that these alterations took place to a great extent to meet the high N requirements by the coffee fruit. Finally, our results indicate that the ability of coffee trees of avoiding the down-regulation of photosynthesis makes it to be suited to sustain relatively enhanced photosynthetic rates in a scenario of increasing atmospheric CO_2 concentration.

References

Antunes WC, Pompelli MF, Carretero DM, DaMatta FM (2008) Allometric models for non-destructive leaf area estimation in cofee (*Coffea arabica* and *Coffea canephora*). Annals of Applied Biology 153:33-40.

Ainsworth, EA and Long SP (2005) What have we learned from 15 years of free-air CO_2 enrichment (FACE)? A meta-analytic review of the responses of photosynthesis, canopy properties and plant production to rising CO2. New Phytologist 165:351–372.

Ainsworth EA, Bush DR (2011) Carbohydrate export from the leaf: a highly regulated process and target to enhance photosynthesis and productivity. Plant Physiology 155:64-69.

Araújo WL, Tohge T, Ishizaki K, Leaver CJ, Fernie AR (2011) Protein degradation: an alternative respiratory substrate for stressed plants. Trends in Plant Science 16:489–498.

Batista KD, Araújo WL, Antunes WC, Cavatte PC, Moraes GABK, Martins SCV, DaMatta FM (2012) Photosynthetic limitations in coffee plants are chiefly governed by diffusive factors. Trees 26:459–468.

Ben-Dor A, R Shamir, and Z Yakhini (1999) Clustering gene expression patterns. Journal of Computational Biology 6:281-297.

Broeckling CD, Huhman DV, Farag MA, Smith JT, May GD (2005) Metabolic profiling of *Medicago truncatula* cell cultures reveals the effects of biotic and abiotic elicitors on metabolism. Journal of Experimental Botany 56:323–336.

Cannell MGR (1971) Effects of fruiting, defoliation and ring-barking on the accumulation and distribution of dry matter in branches of *Coffea arabica* L. in Kenya. Experimental Agriculture 7: 63-74.

Cannell MGR (1975) Crop physiological aspects of coffee bean yield: a review. Journal of Coffee Research 5:7-20.

Cannell MGR (1976) Crop physiological aspects of coffee bean yield: a review. Kenya Coffee 41:145-253.

Chaves ARM, Martins SCV, Batista KD, Celin EF, DaMatta FM (2012) Varying leaf-to-fruit ratios affect branch growth and dieback, with little to no effect on photosynthesis, carbohydrate or mineral pools, in different canopy positions of field-grown coffee trees. Experimental and Environmental Botany 77:207–218.

DaMatta FM, Cunha RL, Antunes WC, Martins SCV, Araújo WL, Fernie AR, Moraes, GABK (2008) In field-grown coffee trees source-to-sink manipulation alters photosynthetic rates, independently of carbon metabolism, via alterations in stomatal function. New Phytologist 178:348-357.

DaMatta FM, Ronchi CP, Maestri M, Barros RS. 2010. Coffee: environment and crop physiology. In: DaMatta FM, ed. Ecophysiology of tropical tree crops, New York: Nova Science Publishers 181-216.

DaMatta FM, Godoy AG, Menezes-silva PE, Martins SCV, Sanglard LMPV, Morais LE, Torre-Neto A, Ghini R (2016) Sustained enhancement of photosynthesis in coffee trees grown under free-air CO_2 enrichment conditions: disentangling the contributions of stomatal, mesophyll, and biochemical limitations. Journal of Experimental Botany 167:341-352.

De Kauwe MG, Lin YS, Wright IJ, Medlyn BE, Kristine Y. Crous KY, Ellsworth DS, Maire V, I. Prentice IC, Atkin OK, Rogers A, Niinemets Ü, Serbin SP, Meir P, Uddling J, Togashi HF, Tarvainen L, Weerasinghe LK, Evans BJ, Ishida FY, Domingues TF (2016) A test of the 'one-point method' for estimating maximum carboxylation capacity from field-measured, light-saturated photosynthesis. New Phytologist, in press.

Eveland AL, Jackson DP (2012) Sugars, signalling, and plant development. Journal of Experimental Botany 63:3367–3377.

Fernie AR, Roscher A, Ratcliffe RG, Kruger NJ (2001) Fructose-2,6-bisphosphate activates pyrophosphate: fructose-6-phosphate 1-phosphotransferase and increases triose phosphate to hexose phosphate cycling in heterotrophic cells. Planta 212:250-263.

Fernie AR, Aharoni A, Willmitzer L, Stitt M, Tohge T, Kopka J, Caroll AJ, Saito K, Fraser PD, DeLuca V (2011) Recommendations for reporting metabolite data. Plant Cell 23:2477-2482.

Flexas J, Barbour MM, Brendel O, Cabrera HM, Carriquí M, Díaz-Espejo A, Douthe C, Dreyer E, Ferrio JP, Gago J (2012) Mesophyll diffusion conductance to CO2: An unappreciated central player in photosynthesis. Plant Science 193-194:70-84.

Florian A, Araújo WL, Fernie AR (2013) New insights into photorespiration obtained from metabolomics. Plant Biology 15:656-666.

Fortunato AS, Lidon FC, Batista-Santo P, Leitão AE, Pais IP, Ribeiro AI, Ramalho JC (2010) Biochemical and molecular characterization of the antioxidative system of *Coffea* sp under cold conditions in genotypes with contrasting tolerance. Journal of Plant Physiology 167:333-342.

Foyer CH, Shigeoka S (2011) Understanding oxidative stress and antioxidant functions to enhance photosynthesis. Plant Physiology 155:93-100.

Foyer CH, Neukermans J, Queval G, Noctor G, Harbinson J (2012) Photosynthetic control of electron transport and the regulation of gene expression. Journal of Experimental Botany 63:1637-1661.

Franck N, Vaast P, Génard M, Dauzat J (2006) Soluble sugars mediate sink feedback down-regulation of leaf photosynthesis in field-grown *Coffea arabica*. Tree Physiology 26:517-525.

Gandin A, Lapointe L, Dizengremel P (2009) The alternative respiratory pathway allows sink to cope with changes in carbon availability in the sink-limited plant *Erythronium americanum*. Journal of Experimental Botany 60:4235-4238.

Gibon Y, Vigeolas H, Tiessen A, Geigenberger P, Stitt M (2002) Sensitive and high throughput metabolite assays for inorganic pyrophosphate, ADPGlc, nucleotide phosphates, and glycolytic intermediates based on a novel enzymic cycling system. Plant Journal 30:221-235.

Gibon Y, Blaesing OE, Hannemann J, Carillo P, Höhne M, Hendriks JHM, Palacios N, Cross J, Selbig J, Stitt, M (2004) A robot-based platform to measure multiple enzyme activities in Arabidopsis using a set of cycling assays: comparison of changes of enzyme activities and transcript levels 4-during diurnal cycles and in prolonged darkness. Plant Cell 16:3305-3325.

Iglesias DJ, Lliso I, Tadeo FR, Talon M (2002) Regulation of photosynthesis through source:sink imbalance in citrus is mediated by carbohydrate content in leaves. Physiologia Plantarum 116:563-572.

Izumi M, Hidema J, Makino A, Ishida H (2013) Autophagy contributes to nighttime energy availability for growth in Arabidopsis. Plant Physiology 161:1682–1693.

Jenner HL, Winning BM, Millar AH, Tomlinson KL, Leaver CJ, Hill AS (2001) NAD malic enzyme and the control of carbohydrate metabolism in potato tubers. Plant Physiology 126:1139-1149.

Kock, KE (1996) Carbohydrate-modulated gene expression in plants. Annual Review of Plant Physiology and Plant Molecular Biology 47:509-540.

Kopka J, Schauer N, Krueger S, Birkemeyer C, Usadel B, Bergmuller E, Dormann P, Weckwerth W, Gibon Y, Stitt M, Willmitzer L, Fernie AR, Steinhauser D (2005) GMD@CSB.DB: the Golm metabolome database. Bioinformatics 21:1635-1638.

Lehmann S, Funck D, Szabados L, Rentsch D (2010) Proline metabolism and transport in plant development. Amino Acids 39:949–962.

Livak KJ, Schmittgen TD (2001). Analysis of relative gene expression data using real-time quantitative PCR and the 2(-Delta Delta C(T)) method. Methods 25:402–408.

Lisec J, Schauer N, Kopka J, Willmitzer L, Fernie AR (2006) Gas chromatography mass spectrometry-based metabolite profiling in plants. Nature Protocols 1:387-396.

Lloyd J, Grace J, Miranda A, Meir P, Wong S, Miranda H, Wright I, Gash J & McIntyre J (1995) A simple calibrated model of Amazon rainforest productivity based on leaf biochemical properties. Plant, Cell and Environment 18:1129-1145.

Lobo AKM, de Oliveira MM, Lima NMC, Machado EC, Ribeiro RV, Silveira JAG (2015) Exogenous sucrose supply changes sugar metabolism and reduces photosynthesis of sugarcane through the down-regulation of rubisco abundance and activity. Journal of Plant Physiology 179:113-121.

Logan BE, Hamelers B, Rozendal R, Schröder U, Keller J, Freguia S, Aelterman P, Verstraete W, Rabaey K (2006) Microbial fuel cells: methodology and technology. Environmental Science and Technology 40:5181– 5192.

López R, Brossa R, Gil L, Pita P (2015). Stem girdling evidences a trade-off between cambial activity and sprouting and dramatically reduces plant transpiration due to feedback inhibition of photosynthesis and hormone signaling. Frontiers in Plant Science 6:285.

Martins SCV, Galmés J, Molins A, DaMatta FM (2013) Improving the estimation of mesophyll conductance: on the role of electron transport rate correction and respiration. Journal of Experimental Botany 64:3285-3298.

Martins SCV, Galmés J, Cavatte PC, Pereira LF, Ventrella MC, DaMatta FM (2014) Understanding the low photosynthetic rates of sun and shade coffee leaves: bridging the gap on the relative roles of hydraulic, diffusive and biochemical constraints to photosynthesis. Plos One 9: e95571.

Maxwell K, Johnson GN (2000) Chlorophyll fluorescence-a practical guide. Journal of Experimental Botany 51:659–668.

Mazzafera P and Gonçalves KV (1998). Nitrogen compounds in the xylem sap of coffee. Phytochemistry 50:383-386.

Müller-Röber B, La Cognata U, Sonnewald U, Willmitzer L (1994) A truncated version of an ADP-glucose pyrophosphorylase promoter from potato specifies guard cell-selective expression in transgenic plants. Plant Cell 6:601–12.

Nishizawa A, Yabuta Y, Shigeoka S (2008) Galactinol and raffinose constitute a novel function to protect plants from oxidative damage. Plant Physiology 147:1251–1263.

Nunes-Nesi A, Carrari F, Lytovchenko A, Smith AMO, Loureiro ME, Ratcliffe RG, Sweetlove LJ, Fernie AR (2005) Enhanced photosynthetic performance and growth as a consequence of decreasing mitochondrial malate dehydrogenase activity in transgenic tomato plants. Plant Physiology 137:611-622.

Nunes-Nesi A, Carrari F, Gibon Y, Sulpice R, Lytovchenko A, Fisahn J, Graham J, Ratcliffe RG, Sweetlove LJ, Fernie AR (2007) Deficiency of mitochondrial fumarase activity in tomato plants impairs photosynthesis via an effect on stomatal function. Plant Journal 50:1093-1106.

Obata T, Fernie AR (2012) The use of metabolomics to dissect plant responses to abiotic stresses. Cellular and Molecular Life Sciences 69:3225-3243.

Paul MJ, Foyer CH (2001) Sink regulation of photosynthesis. Journal of Experimental Botany 52:1383-1400.

Paul MJ, Pellny K (2003) Carbon metabolite feedback regulation of leaf photosynthesis and development. Journal of Experimental Botany 54:539-547.

Piques M, Schulze WX, Hohne M, Usadel B, Gibon Y, Rohwer J, Stitt M. (2009) Ribosome and transcript copy numbers, polysome occupancy and enzyme dynamics in Arabidopsis Molecular Systems Biology 5:314.

Pompelli MF, Martins SCV, Antunes WC, Chaves ARM, DaMatta FM (2010) Photosynthesis and photoprotection in coffee leaves is affected by nitrogen and light availabilities in winter conditions. Journal of Plant Physiology 167:1052-1060.

Praxedes SC, DaMatta FM, Loureiro ME, Ferrão MAG, Cordeiro AT (2006) Effects of long-term soil drought on photosynthesis and carbohydrate metabolism in mature robusta cofee (*Coffea canephora* Pierre var. *kouillou*) leaves. Environmental and Experimental Botany 56:263-273.

Ronchi CP, DaMatta FM, Batista KD, Moraes GABK, Loureiro ME, Ducatti C (2006) Growth and photosynthetic down-regulation in *Coffea arabica* in response to restricting root volume. Functional Plant Biology 33:1013-1023.

Rolland F, Baena-Gonzalez E, Sheen J (2006) Sugar sensing and signaling in plants: conserved and novel mechanisms. Annual Review of Plant Biology 57:675–709.

Schauer N, Steinhauser D, Strelkov S, Schomburg D, Allison G, Moritz T, Lundgren K, Roessner U, Forbes MG, Willmitzer L, Fernie AR, Kopka J (2005) GC-MS libraries for the rapid identification of metabolites in complex biological samples. FEBS Letters 579:1332-1337.

Sheen J (1990) Metabolic repression of transcription in plants. Plant Cell 10:1027-1038.

Stitt M, von Schaewen A, Willmitzer L (1991) “Sink” regulation of photosynthetic metabolism in transgenic tobacco plants expressing yeast invertase in their cell wall involves a decrease of the Calvin-cycle enzymes and an increase of glycolytic enzymes. Planta 183:40–50.

Smith AM, Stitt M (2007) Coordination of carbon supply and plant growth. Plant, Cell and Environment 30:1126–1149.

Sulpice R, Tschoep H, vonKorff M, Bussis D, Usadel B, Hohne M, Witucka-Wall H, Altmann T, Stitt M, Gibon Y (2007) Description and applications of a rapid and

sensitive non-radioactive microplate-based assay for maximal and initial activity of D-ribulose-1,5-bisphosphate carboxylase/oxygenase. Plant, Cell and Environment 30:1163-1175.

Urban L, Léchaudel M, Lu P (2004) Effect of fruit load and girdling on leaf photosynthesis in *Magnifera indica* L. Journal of Experimental Botany 55:2075-2085.

Vaast P, Angrand J, Franck N, Dauzat J, Génard M (2005) Fruit load and branching-barking affect carbon allocation and photosynthesis of leaf and fruit of *Coffea arabica* in the field. Tree Physiology 25:753-760.

Valentini R, Epron D, De Angelis P, Matteucci G, Dreyer E (1995) *In situ* estimation of net CO_2 assimilation, photosynthetic electron flow and photorespiration in Turkey oak (*Q. cerris* L.) leaves: diurnal cycles under different levels of water supply. Plant, Cell and Environment 18:631–640.

van Dongen JT, Gupta KJ, Ramírez-Aguilar SJ, Araújo WL, Nunes-Nesi A, Fernie AR (2011) Regulation of respiration in plants: A role for alternative metabolic pathways. Journal of Plant Physiology 168:1434-1443.

Wilkinson S, Davies WJ (2008) Manipulation of the apoplastic pH of intact plants mimics stomatal and growth responses to water availability and microclimatic variation. Journal of Experimental Botany 59:619–631.

Wilson KB, Baldocchi DD, Hanson PJ (2000) Spatial and seasonal variability of photosynthetic parameters and their relationship to leaf nitrogen in a deciduous forest. Tree Physiology 20:565–578.

Xu M, Duan W, Fan PG, Wu BH, Wang LJ, Ma L, Li SH (2014) Low sink-induced stomatal closure alters photosynthetic rates of source leaves in beans as dependent on H_2O_2 and ABA accumulation in guard cells. Russian Journal of Plant Physiology 61:397-408.

Zhang SQ, Outlaw Jr WH (2001) The guard-cell apoplast as a site of abscisic acid redistribution in *Vicia faba* L. Plant, Cell and Environment 24:347–356.

Tables

Table 1 - The effect of varying source-to-sink ratios [high (HSS), intermediate (ISS) and low (LSS)] on Calvin cycle enzyme activities (μmol min^{-1} g^{-1} FW) at 12:00 h. No significant differences among treatments were found using the Tukey's test at $P \leq 0.05$. $n = 7 \pm$ SE.

Enzymes	HSS	ISS	LSS
RuBisCO(Initial)	0.92 ± 0.07	0.79 ± 0.05	0.80 ± 0.14
RuBisCO (Total)	1.13 ± 0.07	1.04 ± 0.05	0.95 ± 0.14
RuBisCO activation state	82.2 ± 6.80	76.2 ± 4.40	83.8 ± 4.90
PGK	3.96 ± 0.30	4.35 ± 0.27	3.66 ± 0.32
NADPH-GAP3PDH	1.42 ± 0.14	1.48 ± 0.08	1.09 ± 0.16
TPI	122 ± 3.00	121 ± 5.10	118 ± 5.60

Table S1. Designed primers.

Description	Direction	Primer	Tm*	Amplicon
Alkaline invertase	Foward	CAACCTGTTGGCACAATCGCTGC	59.89	94
	Reverse	GAGCACTTGGCACAAAGTCTCGTACA	60.52	
Vacuolar invertase	Foward	CGCCAATCGTTCTCTTACTCTGCC	59.99	113
	Reverse	GTCTACTTTGACCCGAGGACCGAGA	59.72	
Cell wall invertase	Foward	CCGTACCTGATAGAATGGGTCAAATCGC	60.87	72
	Reverse	TGACTCCGACTCCAGAGAACAAAATCAAT	60.12	
Sucrose-phosphate synthase	Foward	TGGAGTTACGGTGAACCCACTGAGATG	60.29	143
	Reverse	GCCAAAAGGAATGCGAATAAGATAAGCC	59.87	
RuBisCO large subunity	Foward	GGCTTTGTTGATTTACTGCGTGATGATTT	59.38	105
	Reverse	GGTATAACACCTGGTAGAGAGACCCAATCT	59.89	
RuBisCO small subunity	Foward	GGACTGAAGAAGTACGAGACTTTGTCATAT	59.16	98
	Reverse	CCAAGCAAGGAACCCATCCACTGC	59.85	
Sucrose synthase	Foward	GAAGGACGCATCAAAGCCCATTATTTTC	59.21	147
	Reverse	TTCACATCGTTGTAACCTGCCACCACA	60.14	
ADP-glucose pyrophosphorylase	Foward	ACTCATTTTGTCTGGAGATCAACTTTACCG	59.72	154
	Reverse	GCCTCTGCTGTCAATCTTCACAAGTC	59.88	
Actin	Foward	TGCTAGTGGTCGGACAACAGGTATAG	59.16	110
	Reverse	AGTCAAGACGGAGGATGGCATGTG	59.40	

(*) Melting temperature

Table S2. The effect of varying source-to-sink ratios [high (HSS), intermediate (ISS) and low (LSS)] source-to-sink on time-course of metabolite content.

	06:00 h			12:00 h			18:00 h			00:00 h			06:00 h		
Amino acids	HSS	ISS	LSS	HSS	ISS	LSS	HSS	ISS	LSS	HSS	ISS	LSS	HSS	ISS	LSS
Alanine	0.145 ± 0.006 Aa	0.127 ± 0.012 Ba	0.069 ± 0.004 Ca	0.113 ± 0.005 Acd	0.087 ± 0.005 Bb	0.069 ± 0.004 Ca	0.101 ± 0.003 Ad	0.087 ± 0.004 ABb	0.076 ± 0.006 Ba	0.119 ± 0.004 Abc	0.094 ± 0.003 Bb	0.067 ± 0.003 Ca	0.131 ± 0.003 Aab	0.114 ± 0.006 Ba	0.079 ± 0.008 Ca
Asparagine	0.132 ± 0.008 Aab	0.228 ± 0.048 Ba	0.043 ± 0.010 Ca	0.153 ± 0.016 Aa	0.127 ± 0.016 Ab	0.026 ± 0.003 Ba	0.166 ± 0.017 Aa	0.087 ± 0.015 Bb	0.042 ± 0.004 Ba	0.097 ± 0.010 Ab	0.095 ± 0.014 Ab	0.043 ± 0.006 Ba	0.120 ± 0.014 Aab	0.114 ± 0.014 Ab	0.027 ± 0.008 Ba
Aspartate	0.122 ± 0.008 Aa	0.129 ± 0.009 Aa	0.086 ± 0.010 Ba	0.114 ± 0.005 Aab	0.106 ± 0.005 ABbc	0.086 ± 0.008 Ba	0.101 ± 0.007 Aab	0.090 ± 0.004 Ac	0.097 ± 0.006 Aa	0.106 ± 0.005 Aab	0.113 ± 0.006 Aab	0.093 ± 0.008 Aa	0.096 ± 0.007 Ab	0.101 ± 0.008 Abc	0.060 ± 0.010 Bb
Glutamine	0.067 ± 0.008 ABcd	0.121 ± 0.043 Ab	0.054 ± 0.008 Bb	0.261 ± 0.025 Aa	0.203 ± 0.025 Ba	0.120 ± 0.009 Ca	0.141 ± 0.015 Ab	0.126 ± 0.018 Ab	0.062 ± 0.007 Bb	0.048 ± 0.002 Ad	0.063 ± 0.004 Ac	0.063 ± 0.007 Ab	0.117 ± 0.007 Abc	0.125 ± 0.013 Ab	0.055 ± 0.008 Bb
Glycine	0.108 ± 0.012 ABb	0.120 ± 0.021 Ab	0.070 ± 0.005 Ba	0.398 ± 0.040 Aa	0.364 ± 0.040 Aa	0.158 ± 0.012 Bb	0.083 ± 0.010 Ab	0.087 ± 0.014 Abc	0.088 ± 0.006 Ab	0.073 ± 0.004 Ab	0.067 ± 0.005 Ac	0.069 ± 0.006 Ab	0.112 ± 0.005 Ab	0.100 ± 0.013 Abc	0.094 ± 0.006 Ab
Histidine	0.153 ± 0.018 Ba	0.337 ± 0.138 Aa	0.127 ± 0.018 Ba	0.168 ± 0.011 Aa	0.072 ± 0.011 Ab	0.059 ± 0.012 Aa	0.193 ± 0.047 Aa	0.046 ± 0.010 Bb	0.058 ± 0.026 Ba	0.079 ± 0.016 Aa	0.071 ± 0.018 Ab	0.073 ± 0.013 Aa	0.122 ± 0.040 Aa	0.104 ± 0.034 Ab	0.051 ± 0.010 Aa
Homoserine	0.121 ± 0.003 ABa	0.125 ± 0.005 Aa	0.109 ± 0.006 Ba	0.105 ± 0.004 Ab	0.092 ± 0.004 Bb	0.065 ± 0.006 Cc	0.084 ± 0.006 Ac	0.075 ± 0.003 ABc	0.067 ± 0.002 Bc	0.105 ± 0.004 Ab	0.099 ± 0.002 Ab	0.095 ± 0.006 Ab	0.103 ± 0.004 Ab	0.097 ± 0.004 ABb	0.089 ± 0.003 Bb
Isoleucine	0.173 ± 0.014 Aa	0.179 ± 0.024 Aa	0.116 ± 0.007 Ba	0.121 ± 0.013 Abc	0.090 ± 0.013 Abc	0.120 ± 0.018 Aa	0.141 ± 0.025 Aab	0.051 ± 0.011 Bc	0.035 ± 0.005 Bb	0.094 ± 0.006 Ac	0.093 ± 0.011 Ab	0.069 ± 0.010 Ab	0.136 ± 0.010 Aab	0.091 ± 0.008 Bb	0.072 ± 0.011 Bb
Leucine	0.169 ± 0.018 Ba	0.230 ± 0.037 Aa	0.128 ± 0.007 Ba	0.048 ± 0.011 Ab	0.047 ± 0.011 Bcd	0.039 ± 0.006 Bbc	0.086 ± 0.010 Ab	0.062 ± 0.005 Bd	0.042 ± 0.007 Bc	0.099 ± 0.005 Ab	0.093 ± 0.008 Ac	0.079 ± 0.008 Ab	0.103 ± 0.005 Ab	0.111 ± 0.003 Ab	0.129 ± 0.014 Aa
Lysine	0.150 ± 0.020 Ba	0.184 ± 0.022 Aa	0.125 ± 0.008 Ba	0.107 ± 0.006 Ab	0.065 ± 0.006 Bcd	0.048 ± 0.004 Bbc	0.088 ± 0.007 Ab	0.048 ± 0.003 Bd	0.046 ± 0.009 Bc	0.105 ± 0.007 Ab	0.084 ± 0.007 Ac	0.079 ± 0.009 Ab	0.114 ± 0.014 Ab	0.125 ± 0.018 Ab	0.123 ± 0.008 Aa
Methionine	0.168 ± 0.024 Aa	0.260 ± 0.089 Aa	0.249 ± 0.100 Aa	0.121 ± 0.003 Aa	0.097 ± 0.003 Ab	0.071 ± 0.011 Abc	0.090 ± 0.004 Aa	0.076 ± 0.004 Ab	0.043 ± 0.008 Ac	0.080 ± 0.007 Aa	0.084 ± 0.006 Ab	0.067 ± 0.011 Abc	0.150 ± 0.005 Aa	0.099 ± 0.013 Ab	0.146 ± 0.015 Ab
Phenylalanine	0.127 ± 0.017 Ba	0.185 ± 0.020 Aa	0.138 ± 0.014 Ba	0.101 ± 0.012 Aab	0.074 ± 0.012 Ab	0.071 ± 0.006 Acd	0.107 ± 0.005 Aab	0.074 ± 0.004 Bb	0.056 ± 0.006 Bd	0.089 ± 0.007 Ab	0.099 ± 0.009 Ab	0.094 ± 0.011 Abc	0.101 ± 0.002 Aab	0.102 ± 0.002 Ab	0.117 ± 0.014 Aab
Proline	0.158 ± 0.005 Ac	0.134 ± 0.011 Aa	0.037 ± 0.006 Ba	0.207 ± 0.005 Aa	0.098 ± 0.005 Bb	0.023 ± 0.004 Ca	0.189 ± 0.009 Aab	0.106 ± 0.008 Bb	0.032 ± 0.002 Ca	0.147 ± 0.011 Ac	0.092 ± 0.009 Bb	0.024 ± 0.002 Ca	0.166 ± 0.009 Abc	0.096 ± 0.011 Bb	0.028 ± 0.004 Ca
Serine	0.133 ± 0.029 Aab	0.134 ± 0.015 Aa	0.101 ± 0.011 Aa	0.103 ± 0.006 Abc	0.082 ± 0.006 ABbc	0.053 ± 0.007 Bb	0.082 ± 0.006 Ac	0.071 ± 0.003 Ab	0.065 ± 0.006 Ab	0.096 ± 0.005 ABc	0.100 ± 0.005 Aab	0.063 ± 0.006 Bb	0.154 ± 0.013 Aa	0.128 ± 0.017 Aa	0.061 ± 0.007 Bb
Tyrosine	0.176 ± 0.015 Ba	0.237 ± 0.057 Aa	0.141 ± 0.006 Ba	0.090 ± 0.019 Ab	0.073 ± 0.019 Ab	0.062 ± 0.007 Abc	0.094 ± 0.014 Ab	0.058 ± 0.011 Ab	0.044 ± 0.004 Ac	0.088 ± 0.005 Ab	0.103 ± 0.014 Ab	0.098 ± 0.009 Aabc	0.099 ± 0.010 Ab	0.112 ± 0.016 Ab	0.105 ± 0.009 Aab
Valine	0.183 ± 0.015 Aa	0.170 ± 0.016 ABa	0.145 ± 0.010 Ba	0.099 ± 0.007 Ac	0.087 ± 0.007 Ab	0.087 ± 0.008 Abc	0.136 ± 0.013 Ab	0.052 ± 0.006 Bc	0.029 ± 0.006 Bd	0.108 ± 0.004 Abc	0.092 ± 0.007 ABb	0.075 ± 0.009 Bc	0.112 ± 0.009 Abc	0.108 ± 0.007 Ab	0.114 ± 0.017 Ab

	06:00 h			12:00 h			18:00 h			00:00 h			06:00 h		
Organic acid	HSS	ISS	LSS	HSS	ISS	LSS	HSS	ISS	LSS	HSS	ISS	LSS	HSS	ISS	LSS
Citrate	0.101 ± 0.010 Aa	0.092 ± 0.004 Ab	0.085 ± 0.013 Aa	0.104 ± 0.007 Aa	0.106 ± 0.007 Aab	0.081 ± 0.007 Ba	0.122 ± 0.006 Aa	0.094 ± 0.007 Bb	0.090 ± 0.003 Ba	0.102 ± 0.005 Ba	0.126 ± 0.007 Aa	0.082 ± 0.010 Ba	0.101 ± 0.007 Aa	0.103 ± 0.004 Ab	0.070 ± 0.010 Ba
Fumarate	0.086 ± 0.004 Ba	0.088 ± 0.003 Ba	0.124 ± 0.003 Aa	0.101 ± 0.005 Aa	0.099 ± 0.005 Aa	0.115 ± 0.011 Aab	0.092 ± 0.003 Ba	0.095 ± 0.004 Ba	0.124 ± 0.006 Aa	0.093 ± 0.005 Ba	0.086 ± 0.006 Ba	0.121 ± 0.006 Aa	0.085 ± 0.007 Aa	0.089 ± 0.005 Aa	0.103 ± 0.005 Ab
2-oxoglutarate	0.100 ± 0.017 Aa	0.076 ± 0.005 Aa	0.085 ± 0.014 Abc	0.101 ± 0.009 Ba	0.110 ± 0.009 Ba	0.179 ± 0.019 Aa	0.103 ± 0.004 Aa	0.075 ± 0.017 Aa	0.093 ± 0.011 Ab	0.052 ± 0.009 Ab	0.075 ± 0.015 Aa	0.050 ± 0.017 Ac	0.128 ± 0.015 Aa	0.116 ± 0.016 Aa	0.106 ± 0.009 Ab
Oxaloacetate	0.138 ± 0.014 Aab	0.184 ± 0.045 Aa	0.043 ± 0.007 Ba	0.167 ± 0.013 Aa	0.100 ± 0.013 Bb	0.024 ± 0.003 Ca	0.120 ± 0.017 Aab	0.077 ± 0.010 ABb	0.027 ± 0.003 Ba	0.112 ± 0.014 Ab	0.097 ± 0.004 Ab	0.042 ± 0.005 Ba	0.130 ± 0.012 Aab	0.116 ± 0.019 Ab	0.029 ± 0.007 Ba
Malate*	111.3 ± 21.1 Ba	119.5 ± 16.5 Bb	152.2 ± 16.6 Aab	120.4 ± 17.8 Bb	148.9 ± 16.0 Aa	165.9 ± 13.6 Aab	94.3 ± 15.4 Ba	165.6 ± 14.9 Bab	170.1 ± 11.6 Aa	116.8 ± 8.4 Aab	124.3 ± 16.6 Ab	150.1 ± 17.3 Ab	112.6 ± 12.1 Ba	145.7 ± 34.2 Bb	173.5 ± 19.5 Aa
Succinate	0.085 ± 0.005 Bb	0.099 ± 0.004 Ab	0.093 ± 0.005 ABc	0.104 ± 0.004 Ba	0.118 ± 0.004 Ba	0.137 ± 0.012 Aa	0.093 ± 0.003 Aab	0.096 ± 0.006 Ab	0.093 ± 0.005 Ac	0.090 ± 0.003 Aab	0.090 ± 0.002 Ab	0.104 ± 0.004 Abc	0.101 ± 0.004 Aa	0.101 ± 0.006 Ab	0.112 ± 0.004 Ab
Trans-caffeonate	0.107 ± 0.005 Aa	0.094 ± 0.007 Ba	0.104 ± 0.004 ABa	0.098 ± 0.003 Aa	0.095 ± 0.003 Aa	0.108 ± 0.005 Aa	0.100 ± 0.005 Aa	0.094 ± 0.004 Aa	0.102 ± 0.005 Aa	0.101 ± 0.002 Aa	0.100 ± 0.005 Aab	0.097 ± 0.004 Aa	0.097 ± 0.003 Aa	0.104 ± 0.005 Aa	0.107 ± 0.005 Aa
Trans-2,5-dimethoxy-Cinnamate	0.102 ± 0.001 Aa	0.100 ± 0.003 Aa	0.100 ± 0.002 Ab	0.097 ± 0.002 Aab	0.097 ± 0.002 Aa	0.100 ± 0.000 Ab	0.095 ± 0.001 Ab	0.099 ± 0.002 Aa	0.099 ± 0.003 Ab	0.099 ± 0.001 Aab	0.099 ± 0.003 Aa	0.092 ± 0.002 Bc	0.098 ± 0.001 Bab	0.102 ± 0.002 ABa	0.106 ± 0.002 Ab
Trans-4-hydroxy-Cinnamate	0.098 ± 0.003 Aa	0.094 ± 0.003 Aab	0.101 ± 0.002 Aabc	0.098 ± 0.003 Aa	0.093 ± 0.003 Aab	0.098 ± 0.005 Abc	0.101 ± 0.002 Aa	0.087 ± 0.004 Bb	0.093 ± 0.004 ABc	0.106 ± 0.003 Aa	0.090 ± 0.003 Bab	0.105 ± 0.004 Aab	0.102 ± 0.003 ABa	0.099 ± 0.003 Ba	0.111 ± 0.005 Aa
Dehydroascorbate	0.088 ± 0.012 Bab	0.080 ± 0.010 Ba	0.123 ± 0.015 Aa	0.090 ± 0.004 Bab	0.091 ± 0.004 Ba	0.140 ± 0.013 Aa	0.078 ± 0.008 Bb	0.094 ± 0.018 ABa	0.119 ± 0.007 b	0.083 ± 0.006 Aab	0.073 ± 0.008 Aa	0.087 ± 0.001 Ab	0.109 ± 0.021 Aa	0.097 ± 0.005 Aa	0.113 ± 0.004 Aab
Trans-ferulate	0.109 ± 0.005 Aa	0.104 ± 0.006 Aa	0.104 ± 0.004 Aab	0.102 ± 0.001 Aa	0.097 ± 0.001 Aab	0.097 ± 0.005 Aab	0.095 ± 0.005 Aa	0.088 ± 0.004 Ab	0.090 ± 0.007 Ab	0.102 ± 0.006 Aa	0.108 ± 0.006 Aa	0.110 ± 0.005 Aa	0.101 ± 0.002 ABa	0.095 ± 0.005 Bab	0.110 ± 0.008 ABa
Galactarate	0.097 ± 0.014 Abc	0.105 ± 0.014 Aab	0.080 ± 0.007 Aa	0.097 ± 0.005 Abc	0.094 ± 0.005 Ab	0.091 ± 0.002 Aa	0.138 ± 0.005 Ba	0.076 ± 0.010 Ab	0.071 ± 0.007 Ba	0.090 ± 0.009 Ac	0.130 ± 0.011 Ba	0.093 ± 0.015 Ba	0.130 ± 0.025 Aab	0.089 ± 0.008 Bb	0.094 ± 0.010 Ba
Maleonate	0.096 ± 0.005 Aab	0.098 ± 0.007 Aab	0.108 ± 0.010 Aa	0.112 ± 0.005 Aa	0.102 ± 0.005 Aa	0.115 ± 0.008 Aa	0.103 ± 0.002 Aab	0.099 ± 0.005 Aab	0.108 ± 0.007 Aa	0.105 ± 0.007 Aa	0.081 ± 0.006 Bb	0.103 ± 0.006 Aa	0.085 ± 0.004 Bb	0.098 ± 0.007 ABab	0.106 ± 0.006 Aa
Quinate	0.108 ± 0.002 Aa	0.102 ± 0.002 Aa	0.089 ± 0.003 Bbc	0.100 ± 0.004 Aab	0.092 ± 0.004 Bb	0.097 ± 0.005 ABab	0.101 ± 0.002 Aab	0.101 ± 0.001 Aa	0.088 ± 0.004 Bc	0.103 ± 0.001 Aab	0.099 ± 0.003 Aab	0.089 ± 0.001 Bc	0.100 ± 0.002 Ab	0.105 ± 0.002 Aa	0.100 ± 0.003 Aa
Saccharate	0.092 ± 0.016 Bc	0.129 ± 0.012 Aa	0.083 ± 0.008 Ba	0.081 ± 0.008 Ac	0.101 ± 0.008 Aab	0.102 ± 0.005 Aa	0.131 ± 0.007 Aab	0.093 ± 0.011 Bab	0.074 ± 0.005 Ba	0.095 ± 0.008 ABbc	0.127 ± 0.011 Aab	0.089 ± 0.013 Ba	0.161 ± 0.032 Aa	0.092 ± 0.010 Bb	0.082 ± 0.006 Ba
Hydrocaffeonate	0.104 ± 0.003 Aa	0.098 ± 0.003 Aa	0.104 ± 0.003 Aa	0.099 ± 0.005 Aa	0.096 ± 0.005 Aa	0.103 ± 0.004 Aa	0.098 ± 0.005 Aa	0.095 ± 0.004 Aa	0.103 ± 0.007 Aa	0.099 ± 0.002 Aa	0.096 ± 0.005 Aa	0.099 ± 0.003 Aa	0.095 ± 0.005 Ba	0.098 ± 0.005 ABa	0.110 ± 0.005 Aa
3-(4-hydroxyphenyl)-Lactate	0.089 ± 0.002 Ca	0.104 ± 0.006 Bab	0.136 ± 0.003 Aa	0.085 ± 0.005 Ba	0.098 ± 0.005 Bab	0.114 ± 0.008 Ab	0.096 ± 0.001 Ba	0.092 ± 0.004 Bb	0.113 ± 0.005 Ab	0.095 ± 0.004 Ba	0.112 ± 0.004 Aa	0.124 ± 0.008 Aab	0.088 ± 0.004 Ba	0.100 ± 0.005 Bab	0.120 ± 0.007 Ab

	06:00 h			12:00 h			18:00 h			00:00 h			06:00 h		
Sugar	HSS	ISS	LSS	HSS	ISS	LSS	HSS	ISS	LSS	HSS	ISS	LSS	HSS	ISS	LSS
Cellobiose	0.104 ± 0.003	0.097 ± 0.002	0.108 ± 0.003	0.093 ± 0.002	0.104 ± 0.002	0.105 ± 0.003	0.095 ± 0.003	0.105 ± 0.002	0.103 ± 0.005	0.108 ± 0.004	0.095 ± 0.004	0.101 ± 0.003	0.092 ± 0.003	0.092 ± 0.003	0.103 ± 0.006
	ABab	Bab	Aa	Bc	Aa	Aa	Bbc	Aa	ABa	Aa	Bab	ABa	Bc	Bb	Aa
Galactose	0.124 ± 0.009	0.111 ± 0.016	0.068 ± 0.008	0.103 ± 0.004	0.116 ± 0.004	0.101 ± 0.012	0.095 ± 0.004	0.127 ± 0.011	0.094 ± 0.003	0.108 ± 0.020	0.093 ± 0.004	0.097 ± 0.032	0.100 ± 0.008	0.147 ± 0.015	0.080 ± 0.012
	Aa	Aab	Ba	Aa	Aab	Aa	Aa	Aab	Aa	Aa	Ab	Aa	Ba	Aa	Ba
Glucose	0.103 ± 0.008	0.076 ± 0.010	0.048 ± 0.004	0.086 ± 0.018	0.174 ± 0.018	0.148 ± 0.012	0.085 ± 0.005	0.146 ± 0.020	0.122 ± 0.004	0.078 ± 0.010	0.078 ± 0.010	0.052 ± 0.009	0.094 ± 0.008	0.132 ± 0.010	0.054 ± 0.008
	Aa	ABc	Bb	Ba	Aa	Aa	Ba	Aab	Aa	Aa	Ac	Ab	Ba	Ab	Cb
Maltose	0.070 ± 0.002	0.129 ± 0.011	0.083 ± 0.017	0.136 ± 0.005	0.084 ± 0.005	0.066 ± 0.004	0.061 ± 0.002	0.071 ± 0.005	0.081 ± 0.008	0.096 ± 0.007	0.165 ± 0.018	0.211 ± 0.013	0.090 ± 0.005	0.110 ± 0.003	0.276 ± 0.025
	Bbc	Ab	Bc	Aa	Bcd	Bc	Ac	Ad	Ac	Cb	Ba	Ab	Bbc	Bbc	Aa
Maltotriose	0.093 ± 0.005	0.084 ± 0.006	0.105 ± 0.004	0.103 ± 0.003	0.089 ± 0.003	0.100 ± 0.007	0.091 ± 0.004	0.079 ± 0.002	0.106 ± 0.005	0.092 ± 0.007	0.107 ± 0.009	0.118 ± 0.002	0.092 ± 0.003	0.101 ± 0.004	0.114 ± 0.006
	ABa	Bbc	Aab	Aa	Abc	Ab	ABa	Bc	Aab	Ba	ABa	Aa	Ba	ABab	Aab
Melezitose	0.092 ± 0.005	0.105 ± 0.004	0.086 ± 0.003	0.125 ± 0.006	0.141 ± 0.006	0.088 ± 0.005	0.122 ± 0.009	0.117 ± 0.008	0.104 ± 0.005	0.087 ± 0.003	0.098 ± 0.004	0.101 ± 0.005	0.088 ± 0.002	0.088 ± 0.004	0.086 ± 0.015
	ABb	Abc	Ba	Aa	Aa	Ba	Aa	ABb	Ba	Ab	Ac	Aa	Ab	Ac	Aa
Raffinose	0.098 ± 0.002	0.099 ± 0.002	0.083 ± 0.002	0.102 ± 0.001	0.097 ± 0.001	0.108 ± 0.004	0.103 ± 0.001	0.100 ± 0.001	0.102 ± 0.003	0.102 ± 0.002	0.103 ± 0.001	0.088 ± 0.003	0.096 ± 0.004	0.100 ± 0.003	0.094 ± 0.005
	Aa	Aa	Bc	ABa	Ba	Aa	Aa	Aa	Aa	Aa	Aa	Bbc	Aa	Aa	Ab
Idose	0.088 ± 0.014	0.099 ± 0.005	0.086 ± 0.009	0.110 ± 0.009	0.109 ± 0.009	0.121 ± 0.023	0.117 ± 0.010	0.092 ± 0.009	0.067 ± 0.009	0.105 ± 0.011	0.113 ± 0.009	0.092 ± 0.009	0.073 ± 0.012	0.107 ± 0.009	0.088 ± 0.007
	Aab	Aa	Ab	Aa	Aa	Aa	Aa	ABa	Bb	Aa	Aa	Aab	Bb	Aa	ABb
Sorbose	0.092 ± 0.017	0.094 ± 0.008	0.040 ± 0.009	0.089 ± 0.009	0.155 ± 0.009	0.151 ± 0.017	0.101 ± 0.017	0.140 ± 0.016	0.131 ± 0.009	0.087 ± 0.020	0.102 ± 0.011	0.055 ± 0.002	0.080 ± 0.011	0.146 ± 0.034	0.055 ± 0.010
	Aa	Ac	Bb	Ba	Aa	Aa	Aa	Aab	Aa	ABa	Abc	Bb	Ba	Aab	Bb
Sucrose*	59.4 ± 2.5	69.4 ± 3.4	38.9 ± 2.6	86.8 ± 3.9	77.0 ± 2.5	79.2 ± 6.2	73.5 ± 6.3	78.3 ± 2.8	76.5 ± 2.7	74.9 ± 2.1	67.6 ± 3.5	49.2 ± 2.8	69.8 ± 2.2	62.7 ± 1.4	46.1 ± 4.6
	Bc	Abc	Cc	Aa	Bab	ABa	Ab	Aa	Aa	Ab	Ac	Bb	Ab	Ac	Bbc
Trehalose	0.113 ± 0.002	0.093 ± 0.007	0.046 ± 0.003	0.133 ± 0.010	0.130 ± 0.010	0.108 ± 0.012	0.115 ± 0.003	0.110 ± 0.005	0.100 ± 0.006	0.096 ± 0.003	0.080 ± 0.006	0.068 ± 0.002	0.097 ± 0.006	0.091 ± 0.004	0.076 ± 0.007
	Abc	Bbc	Cc	Aa	Aa	Ba	Aab	Ab	Aa	Ac	ABc	Bb	Abc	ABc	Bb
Sugar alcohols															
Erythritol	0.100 ± 0.008	0.095 ± 0.008	0.098 ± 0.006	0.128 ± 0.009	0.101 ± 0.009	0.092 ± 0.007	0.104 ± 0.006	0.091 ± 0.006	0.088 ± 0.002	0.121 ± 0.010	0.100 ± 0.002	0.089 ± 0.003	0.126 ± 0.010	0.087 ± 0.004	0.068 ± 0.004
	Ac	Aa	Aa	Aa	Ba	Ba	Abc	Aa	Aa	Aab	Ba	Ba	Aa	Ba	Bb
Glycerol	0.115 ± 0.004	0.128 ± 0.008	0.080 ± 0.005	0.137 ± 0.002	0.089 ± 0.002	0.080 ± 0.004	0.127 ± 0.005	0.106 ± 0.008	0.063 ± 0.005	0.152 ± 0.005	0.085 ± 0.004	0.075 ± 0.008	0.124 ± 0.003	0.084 ± 0.006	0.076 ± 0.003
	Ac	Aa	Ba	Aab	Bc	Ba	Abc	Bb	Cb	Aa	Bc	Bab	Abc	Bc	Bab
Myo-Inositol	0.103 ± 0.005	0.120 ± 0.004	0.124 ± 0.003	0.101 ± 0.002	0.094 ± 0.002	0.095 ± 0.009	0.086 ± 0.003	0.090 ± 0.003	0.073 ± 0.003	0.127 ± 0.009	0.105 ± 0.003	0.103 ± 0.002	0.106 ± 0.008	0.111 ± 0.004	0.106 ± 0.006
	Bb	Aa	Aa	Abc	Ab	Ab	ABc	Ab	Bc	Aa	Bab	Bb	Ab	Aa	Ab
Galactinol	0.104 ± 0.002	0.100 ± 0.003	0.073 ± 0.006	0.102 ± 0.003	0.103 ± 0.003	0.087 ± 0.006	0.105 ± 0.002	0.106 ± 0.002	0.079 ± 0.003	0.102 ± 0.001	0.101 ± 0.003	0.082 ± 0.003	0.102 ± 0.003	0.104 ± 0.003	0.082 ± 0.007
	Aa	Aa	Bb	Aa	Aa	Ba	Aa	Aa	Bab	Aa	Aa	Bab	Aa	Aa	Bab
Polyamines															
Ornithine	0.117 ± 0.019	0.165 ± 0.037	0.098 ± 0.013	0.196 ± 0.024	0.107 ± 0.024	0.081 ± 0.007	0.091 ± 0.011	0.078 ± 0.021	0.071 ± 0.020	0.080 ± 0.007	0.103 ± 0.008	0.081 ± 0.007	0.119 ± 0.019	0.144 ± 0.066	0.085 ± 0.012
	Ab	Aa	Aa	Aa	Bab	Ba	Ab	Ab	Aa	Ab	Aab	Aa	Ab	Aab	Aa
Tyramine	0.096 ± 0.008	0.102 ± 0.006	0.147 ± 0.005	0.094 ± 0.005	0.103 ± 0.005	0.122 ± 0.006	0.084 ± 0.005	0.102 ± 0.001	0.104 ± 0.007	0.086 ± 0.005	0.093 ± 0.006	0.112 ± 0.006	0.081 ± 0.002	0.104 ± 0.005	0.114 ± 0.011
	Ba	Ba	Aa	Ba	Ba	Ab	Ba	ABa	Ac	Ba	Ba	Abc	Ba	Aa	Abc
Putrescine	0.100 ± 0.015	0.109 ± 0.026	0.121 ± 0.009	0.127 ± 0.011	0.140 ± 0.011	0.095 ± 0.007	0.093 ± 0.005	0.111 ± 0.012	0.093 ± 0.004	0.093 ± 0.009	0.073 ± 0.007	0.094 ± 0.010	0.105 ± 0.009	0.096 ± 0.014	0.087 ± 0.006
	Aa	Aab	Aa	ABa	Aa	Ba	Aa	Aab	Aa	Aa	Ac	Aa	Aa	Abc	Aa
Flavonols															
Myricetin	0.101 ± 0.005	0.093 ± 0.006	0.107 ± 0.005	0.091 ± 0.001	0.098 ± 0.001	0.107 ± 0.003	0.097 ± 0.005	0.087 ± 0.003	0.104 ± 0.005	0.098 ± 0.006	0.104 ± 0.005	0.102 ± 0.002	0.094 ± 0.003	0.092 ± 0.003	0.103 ± 0.007
	Aa	Aab	Aa	Ba	ABab	A	ABa	Bb	Aa	Aa	Aa	Aa	Aa	Aab	Aa
Quercetin	0.104 ± 0.002	0.093 ± 0.005	0.110 ± 0.004	0.097 ± 0.006	0.091 ± 0.006	0.082 ± 0.003	0.088 ± 0.006	0.091 ± 0.006	0.116 ± 0.009	0.101 ± 0.005	0.106 ± 0.004	0.110 ± 0.004	0.094 ± 0.004	0.093 ± 0.005	0.101 ± 0.004
	ABa	Bab	Aab	Aab	ABbc	Bc	Bb	Bb	Aa	Aab	Aa	Aab	Aab	Aab	Ab

Different capital letters indicate differences among means within each time point; different lowercase letters indicate differences among means for a given treatment along the day. Means were compared using the Tukey´s test at $P \leq 0.05$. $n = 7 \pm$ SE. Metabolites were quantified using a GC/MS with two exceptions that were marked with an asterisks.

Figure legends

Figure 1. The effect of varying source-to-sink ratios [high (HSS), intermediate (ISS) and low (LSS)] on time-course of net CO_2 assimilation rate, A (A), stomatal conductance, g_s, (B), A x g_s relationship (C), internal CO_2 concentration, C_i (D), photorespiration-to-gross photosynthesis ratio, R_p/A_{gross} (E), maximum apparent carboxylation capacity on a chloroplastic CO_2 concentration basis, V_{cmax} (F) and dark respiration, R_d (G). Different capital letters indicate differences among means within each time point; different lowercase letters indicate differences among means for a given treatment along the day. Means were compared using the Tukey's test at $P \leq 0.05$. $n = 7 \pm$ SE.

Figure 2. The effect of varying source-to-sink ratios [high (HSS), intermediate (ISS) and low (LSS)] on time-course of photochemical quenching coefficient, q_p (A), non-photochemical quenching, NPQ (B), the electron transport rate, ETR (C) and. Different capital letters indicate differences among means within each time point; different lowercase letters indicate differences among means for a given treatment along the day. Means were compared using the Tukey's test at $P \leq 0.05$. $n = 7 \pm$ SE.

Figure 3. The effect of varying source-to-sink ratios [high (HSS), intermediate (ISS) and low (LSS)] on time-course of NAD^+ (A), NADH (B), NADH/NAD^+ ratio (C), $NADP^+$ (D), NADPH (E) and NADPH/$NADP^+$ ratio (F). Different capital letters indicate differences among means within each time point; different lowercase letters indicate differences among means for a given treatment along the day. Means were compared using the Tukey's test at $P \leq 0.05$. $n = 7 \pm$ SE.

Figure 4. The effect of varying source-to-sink ratios [high (HSS), intermediate (ISS) and low (LSS)] on time-course of starch (A), sucrose (B), hexoses (glucose and fructose) (C), total amino acids (D) and protein (E). Different capital letters indicate differences among means within each time point; different lowercase letters indicate differences among means for a given treatment along the day. Means were compared using the Tukey's test at $P \leq 0.05$. $n = 7 \pm$ SE.

Figure 5. The effect of varying source-to-sink ratios [high (HSS), intermediate (ISS) and low (LSS)] on time-course of ADP-glucose pyrophosphorylase (AGPase) (A), SPS, initial activity (B), SPS, total activity (C) and SPS activation state (D). Different capital letters indicate differences among means within each time point; different lowercase letters indicate differences among means for a given treatment along the day. Means were compared using the Tukey's test at $P \leq 0.05$. $n = 7 \pm$ SE.

Figure 6. The effect of varying source-to-sink ratios [high (HSS), intermediate (ISS) and low (LSS)] on time-course of transcript patterns of ADP-glucose pyrophosphorylase (AGPase) (A), RuBisCO small subunit (B), RuBisCO large subunit (C), sucrose-phosphate synthase (SPS) (D), sucrose synthase (SuSy) (E), cell wall invertase (F), vacuolar (G) and alkaline (H) invertases. Different capital letters indicate differences among means within each time point; different lowercase letters indicate differences among means for a given treatment along the day. Means were compared using the Tukey's test at $P \leq 0.05$. $n = 7 \pm$ SE.

Figure 7. The effect of varying source-to-sink ratios [high (HSS), intermediate (ISS) and low (LSS)] on time-course of metabolites relative content. Clusters I, II, III, IV and V reveals varying patterns of metabolite accumulation over the course of the day (see the Results section). Clustering analysis was made by using an internal tool called Cluster Affinity Search Technique (CAST) (Pearson Correlation threshold = 0.8) from the software MultExperiemnt Viewer (MeV). Metabolites were quantified using a GC/MS with one exception that were marked with an asterisk.

Figure S1. The effect of varying source-to-sink ratios [high (HSS), intermediate (ISS) and low (LSS)] on time-course of enolase (ENO) (A), aldolase (ALD) (B), phosphofructokinase (PFK) (C) hexokinase (HK) (D), NAD^+-dependent dehydrogenase NAD^+-MDH (E), sucrose synthase (F), alkaline (G) and acid invertase activity. Different capital letters indicate differences among means within each time point; different lowercase letters indicate differences among means for a given treatment along the day. Means were compared using the Tukey's test at $P \leq 0.05$. $n = 7 \pm$ SE.

Figures

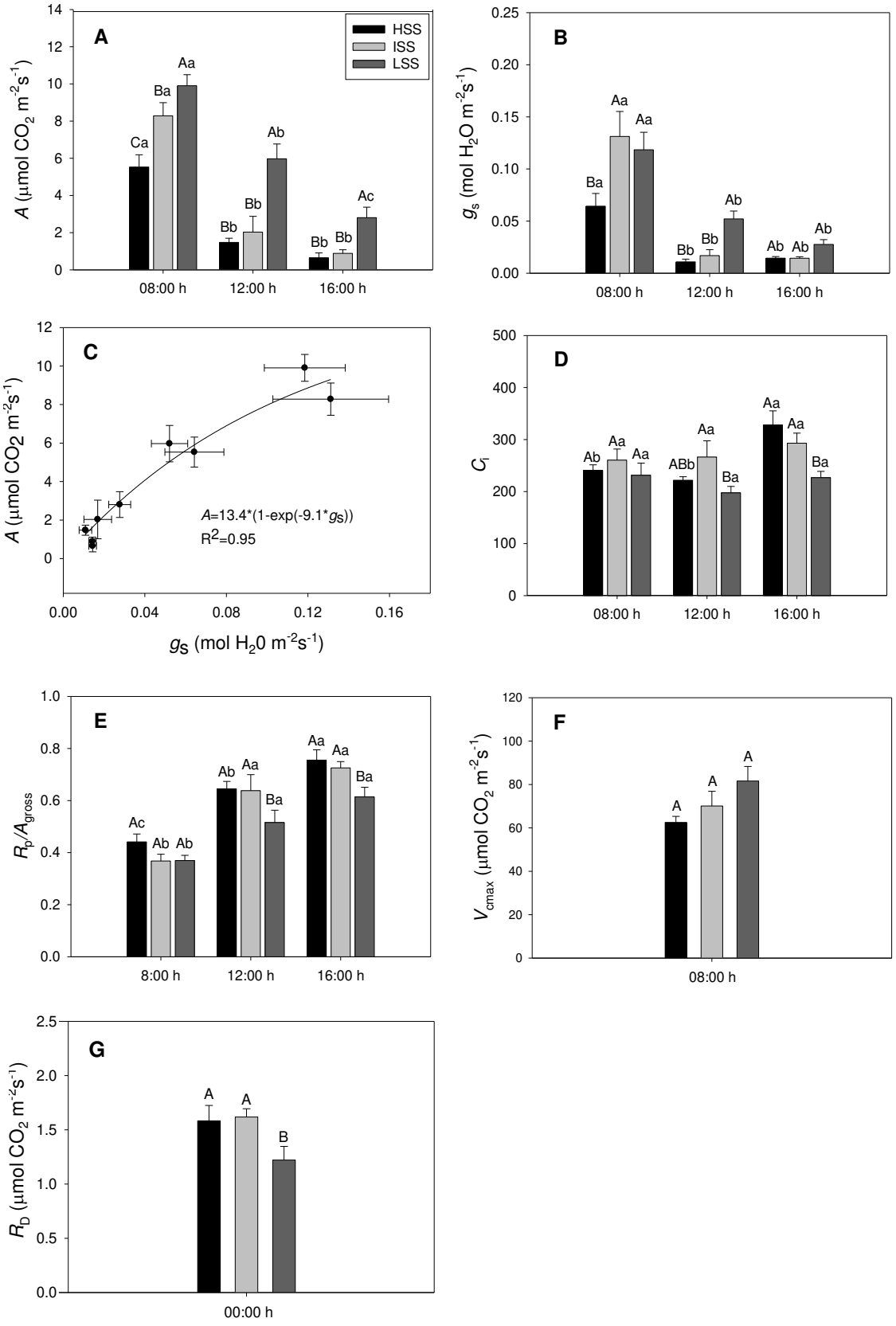

Figure 1

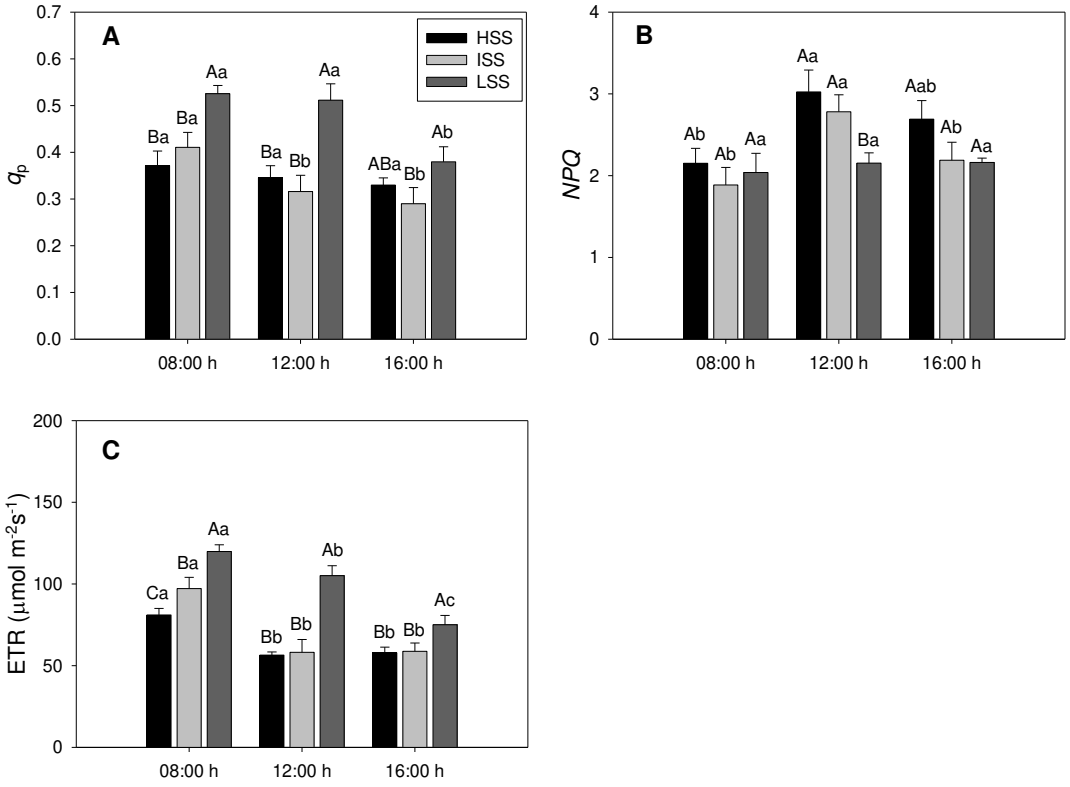
A
HSS
ISS
LSS
q_p
0.7
0.6
0.5
0.4
0.3
0.2
0.1
0.0
Ba
Ba
Aa
Ba
Bb
Aa
ABa
Bb
Ab
08:00 h
12:00 h
16:00 h
B
NPQ
4
3
2
1
0
Ab
Ab
Aa
Aa
Aa
Ba
Aab
Ab
Aa
08:00 h
12:00 h
16:00 h
C
ETR (µmol m^{-2}s^{-1})
200
150
100
50
0
Ca
Ba
Aa
Bb
Bb
Ab
Bb
Bb
Ac
08:00 h
12:00 h
16:00 h

Figure 2

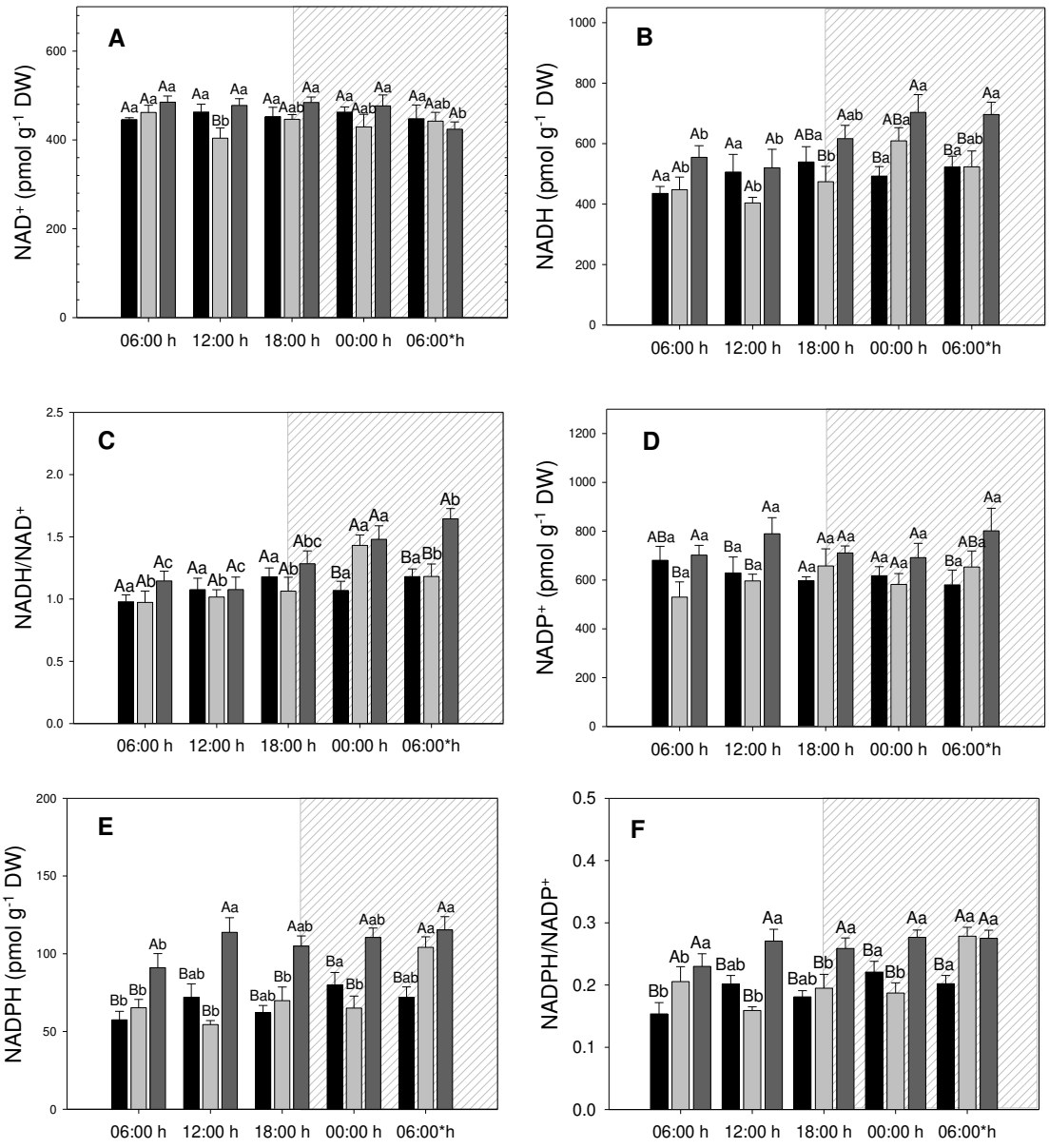
A
NAD+ (pmol g-1 DW)
B
NADH (pmol g-1 DW)
C
NADH/NAD+
D
NADP+ (pmol g-1 DW)
E
NADPH (pmol g-1 DW)
F
NADPH/NADP+
06:00 h
12:00 h
18:00 h
00:00 h
06:00*h

Figure 3

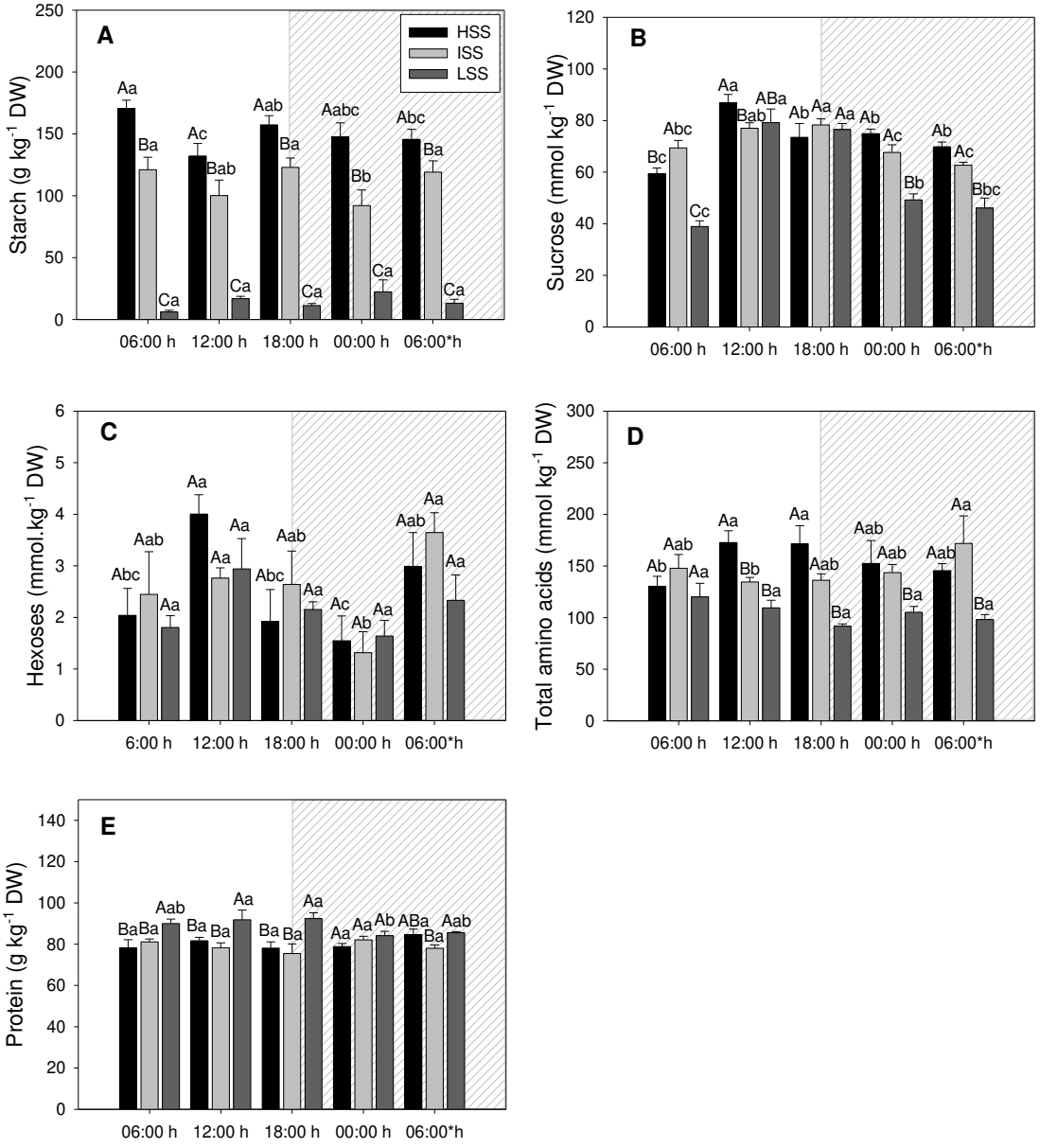
A
HSS
ISS
LSS
Starch (g kg-1 DW)
Aa Ba Ca Ac Bab Ca Aab Ba Ca Aabc Bb Ca Abc Ba Ca
06:00 h 12:00 h 18:00 h 00:00 h 06:00*h
B
Sucrose (mmol kg-1 DW)
Bc Abc Cc Aa Bab ABa Ab Aa Aa Ab Ac Bb Ab Ac Bbc
06:00 h 12:00 h 18:00 h 00:00 h 06:00*h
C
Hexoses (mmol.kg-1 DW)
Abc Aab Aa Aa Aa Aa Abc Aab Aa Ac Ab Aa Aab Aa Aa
6:00 h 12:00 h 18:00 h 00:00 h 06:00*h
D
Total amino acids (mmol kg-1 DW)
Ab Aab Aa Aa Bb Ba Aa Aab Ba Aab Aab Ba Aab Aa Ba
06:00 h 12:00 h 18:00 h 00:00 h 06:00*h
E
Protein (g kg-1 DW)
Ba Ba Aab Ba Ba Aa Ba Ba Aa Aa Aa Ab ABa Ba Aab
06:00 h 12:00 h 18:00 h 00:00 h 06:00*h

Figure 4

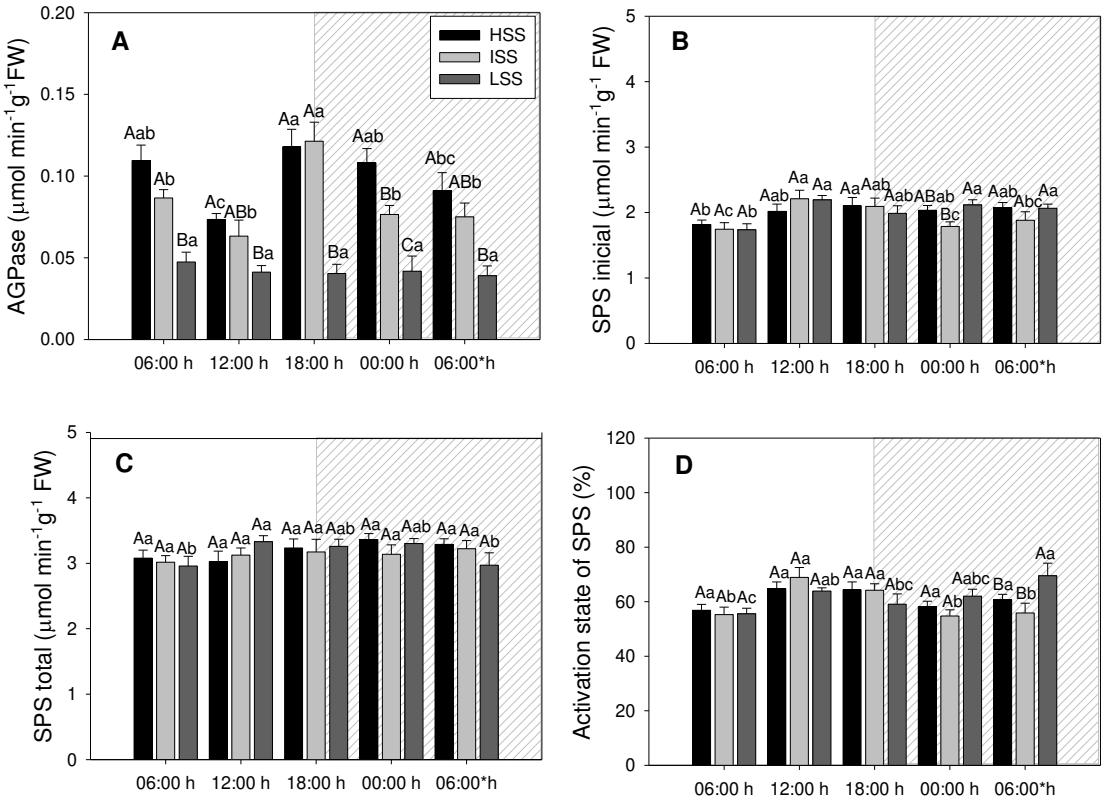
A
HSS
ISS
LSS
AGPase (μmol min-1g-1FW)
0.20
0.15
0.10
0.05
0.00
Aab
Ab
Ba
Ac
ABb
Ba
Aa
Aa
Ba
Aab
Bb
Ca
Abc
ABb
Ba
06:00 h
12:00 h
18:00 h
00:00 h
06:00*h
B
SPS inicial (μmol min-1g-1 FW)
5
4
3
2
1
0
Ab Ac Ab
Aab
Aa
Aa
Aa
Aab
Aab
ABab
Bc
Aa
Aab
Abc
Aa
06:00 h
12:00 h
18:00 h
00:00 h
06:00*h
C
SPS total (μmol min-1g-1 FW)
5
4
3
2
1
0
Aa Aa Ab
Aa Aa Aa
Aa Aa Aab
Aa Aa Aab
Aa Aa Ab
06:00 h
12:00 h
18:00 h
00:00 h
06:00*h
D
Activation state of SPS (%)
120
100
80
60
40
20
0
Aa Ab Ac
Aa
Aa
Aab
Aa Aa
Abc
Aa
Ab
Aabc
Ba
Bb
Aa
06:00 h
12:00 h
18:00 h
00:00 h
06:00*h

Figure 5

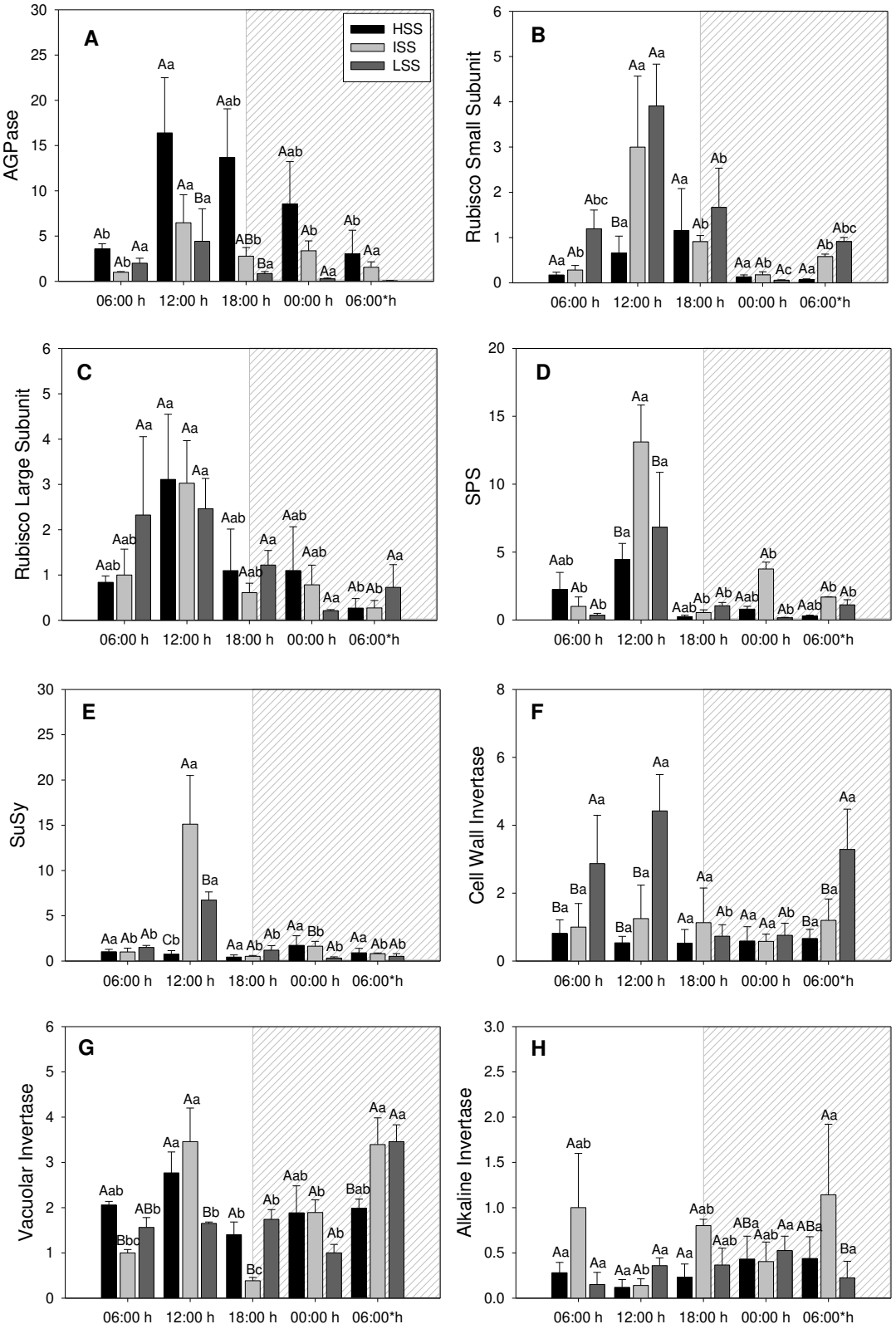
A
AGPase
HSS
ISS
LSS
B
Rubisco Small Subunit
C
Rubisco Large Subunit
D
SPS
E
SuSy
F
Cell Wall Invertase
G
Vacuolar Invertase
H
Alkaline Invertase
06:00 h
12:00 h
18:00 h
00:00 h
06:00*h

Figure 6

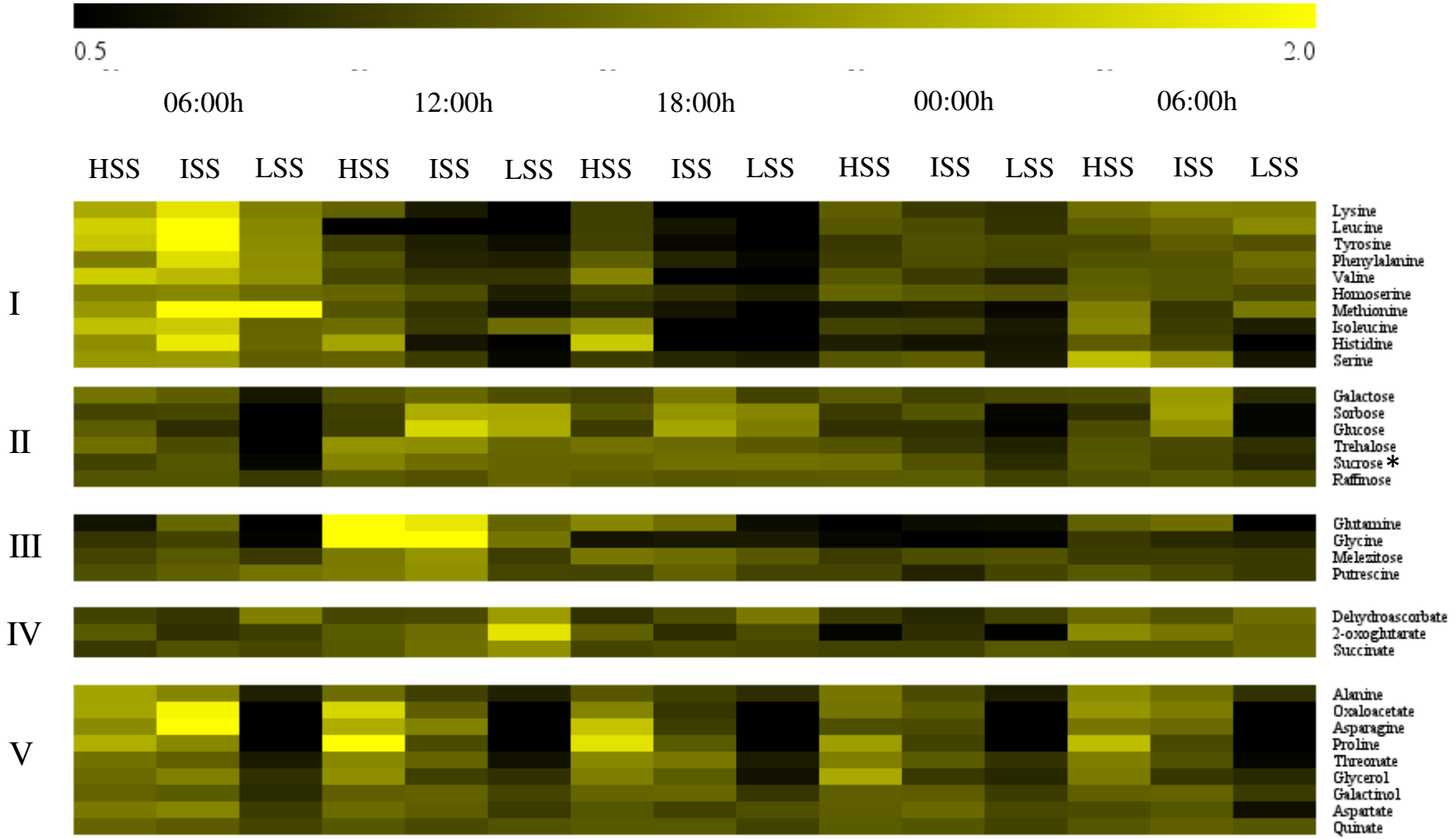
0.5
2.0
06:00h
12:00h
18:00h
00:00h
06:00h
HSS ISS LSS HSS ISS LSS HSS ISS LSS HSS ISS LSS HSS ISS LSS
I
II
III
IV
V
Lysine
Leucine
Tyrosine
Phenylalanine
Valine
Homoserine
Methionine
Isoleucine
Histidine
Serine
Galactose
Sorbose
Glucose
Trehalose
Sucrose *
Raffinose
Glutamine
Glycine
Melezitose
Putrescine
Dehydroascorbate
2-oxoglutarate
Succinate
Alanine
Oxaloacetate
Asparagine
Proline
Threonate
Glycerol
Galactinol
Aspartate
Quinate

Figure 7

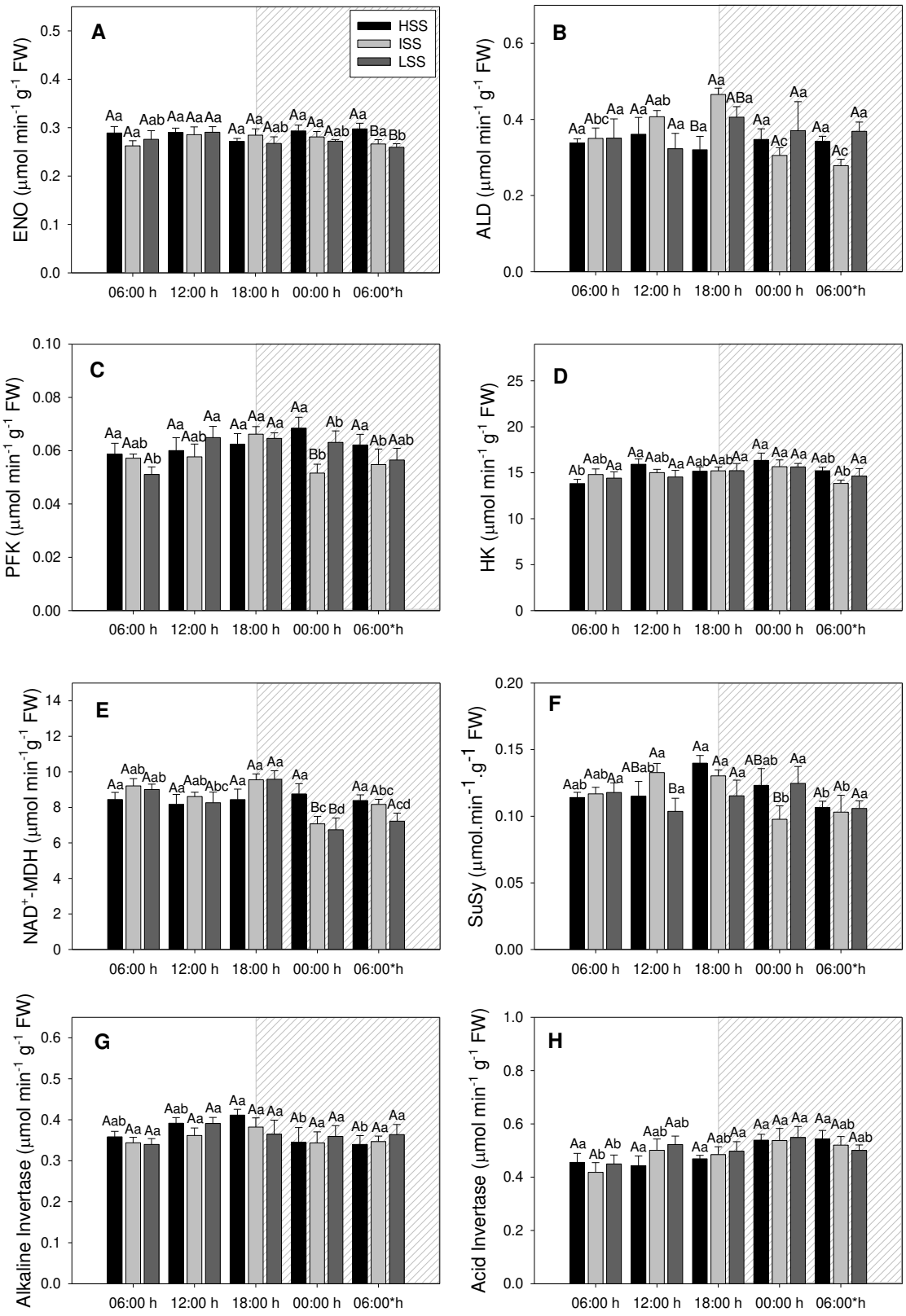
A
HSS
ISS
LSS
ENO (μmol min-1 g-1 FW)
B
ALD (μmol min-1 g-1 FW)
C
PFK (μmol min-1 g-1 FW)
D
HK (μmol min-1 g-1 FW)
E
NAD+-MDH (μmol min-1 g-1 FW)
F
SuSy (μmol.min-1.g-1 FW)
G
Alkaline Invertase (μmol min-1 g-1 FW)
H
Acid Invertase (μmol min-1 g-1 FW)
06:00 h
12:00 h
18:00 h
00:00 h
06:00*h

Figure S1